

Journal of Engineering Research

METHODOLOGY FOR ENERGY EFFICIENCY ANALYSIS AND OPTIMIZATION OF SHIP SYSTEMS USING EXERGY MODELING

Luciana Maria da Silva Suman Jardim

Carlos Belchior

All content in this magazine is licensed under a Creative Commons Attribution License. Attribution-Non-Commercial-Non-Derivatives 4.0 International (CC BY-NC-ND 4.0).



Abstract: In January 2023, the International Maritime Organization (IMO) through Resolution 333 (76), required ships of 400 GT or more engaged in international voyages to comply with the Energy Efficiency Existing Ship Index (EEXI). This study aims to develop a tool for selecting existing technologies that have the greatest impact on CO₂ reduction, aligning vessels with environmental indicators. It is common for ships, even of the same design, to exhibit different performances due to various operations and maintenance. Therefore, it is essential to consider the unique characteristics of each vessel. This paper presents a methodology developed through exergy modeling to identify primary inefficiencies and assess the potential for residual heat recovery in the main combustion engines of an oil tanker that did not meet the EEXI criteria and operates off the Brazilian coast relieving FPSOs. Exergy modeling allows identifying areas of significant energy waste and applying suitable technology. The study concludes that applying the proposed methodology enables a genuine reduction in CO₂ emissions, aligning vessels with IMO's environmental indicators. Despite the longstanding use of exergy in the maritime domain, the method presented here uses exergy as a tool for selecting emission reduction technology, an unexplored territory.

Keywords Ship Emissions; Energy Efficiency, Exergetic Efficiency, Energy Efficiency Existing Ship Index.

INTRODUCTION

Maritime transport is widely acknowledged as the most efficient means of transport when considering the ratio between the volume of cargo carried and the associated CO₂ emissions. As highlighted by the International Maritime Organization (IMO) (IMO,2022), ships accounted for an impressive 90% of the global cargo volume in 2018. However, this

relative efficiency is shadowed by significant challenges in terms of carbon emissions. According to (FABER, J. et al.,2020), (MBM-EG, 2010; ANINK et al. 2011), the maritime transport sector contributed to approximately 2.6% of the total global CO₂ emissions and 2.8% of the CO₂ equivalent emissions.

The (IMO,2022), through the Marpol Convention 73/78, has set ambitious targets to curb emissions in the maritime sector. (FABER, J. et al.,2020), underscores that, notwithstanding the ships' inherent efficiency, emissions have seen a considerable rise, with projections indicating a potential increase of 50% by 2050 unless appropriate measures are put in place. Recognizing this concern, the IMO has set forth targets that encompass a minimum 40% reduction in carbon intensity by 2030 and a minimum 50% cut in the annual total greenhouse gas emissions by 2050, both compared to 2008 levels.

(MBM-EG, 2010) points out that the IMO has crafted strategies to achieve these objectives, which include short, medium, and long-term measures for effective deployment. One of the short-term measures (scheduled between 2023 and 2030) involves the adoption of energy efficiency indicators for existing ships. This proposal stems from the challenge of meeting the CO₂ reduction targets, especially due to the presence of ships in the global fleet built before January 1, 2013, as alluded to in the MEPC 334 (76) document (IMO,2021) issued by the IMO.

The chosen indicator for this purpose is the Energy Efficiency Existing Ship Index (EEXI), also referenced in the Marpol Convention 73/78. Thus, the citations allude to the IMO's commitment to addressing the surge in carbon emissions in maritime transport and the strategies and measures embraced to achieve these aims, with an emphasis on energy efficiency and curbing emissions from the existing fleet.

MOTIVATION

The motivation for this study arose from observing the difficulty in aligning and reducing CO₂ emissions in ships whose original designs were not developed according to the goals set by the IMO. Although maritime transport is the most efficient mode of transportation, the measures imposed by the IMO force shipowners to resort to technologies, often relying on manufacturers' promises of energy reduction that does not always materialize. This occurs mainly because shipowners frequently do not know exactly which equipment, process, or system on the vessel has the greatest loss of energy and exergy efficiency.

This study, through thermodynamic analysis, inherently addresses the peculiar aspects of vessels that influence exergy parameters, such as operation, maintenance, trade (such as vessels with successive docking), design, and systems. Identifying, among the existing technologies, those that provide the highest value in reducing emissions constitutes a significant challenge.

CURRENT LITERATURE REVIEW ON ENERGY AND EXERGY APPLIED TO SHIPS

The energy and exergy analysis of ship energy systems has been a growing area of interest in academic literature due to the need to optimize energy efficiency and reduce CO₂ emissions. Several studies highlight the importance of understanding in detail how energy consumption on ships is generated and how inefficiencies can be addressed.

In the study by Baldi et al. (2014), titled "Energy and exergy analysis of ship energy systems – the case study of a chemical tanker," the authors highlight the importance of understanding in detail how energy consumption on ships is generated. The study proposes a methodology applied to a chemical

tanker, allowing the identification of primary inefficiencies and the evaluation of energy waste flows. Notably, the exergy analysis identified significant potential for waste heat recovery in exhaust gases, representing an exergy flow equivalent to 18% of the engine's output power.

In another study, Trinklein et al. (2019), in "Modelling, Optimization, and Control of Ship Energy Systems Using Exergy Methods," discuss the optimization of ship energy systems using exergy methods. By modelling multiple system domains simultaneously and applying the Second Law of Thermodynamics, the authors demonstrate it is possible to minimize total exergy destruction. This results in lower emissions and fuel costs, leading to more efficient, smaller, and lighter onboard systems.

Waste heat recovery on ships is also addressed by Larsen et al. (2014) in the study "A comparison of advanced heat recovery power cycles in a combined cycle for large ships." The authors compare different waste heat recovery cycles (WHR), concluding that the Organic Rankine Cycle (ORC) has the greatest potential to increase fuel efficiency, despite high global warming potentials and associated hazard levels. In contrast, the steam cycle is less efficient but environmentally benign and proven safe in practical terms.

Baldi et al. (2017), in "Energy and Exergy Analysis of a Cruise Ship," analyse the energy and exergy efficiency of a cruise ship. Through exergy modelling, the study identifies significant areas of energy waste and suggests specific technological improvements to reduce emissions and increase the energy efficiency of onboard systems.

Tran (2019), in the study "Establishment of Energy Efficiency Operational Indicator (EEOI) for ships," presents a numerical model for calculating the EEOI considering environmental navigation conditions. This work highlights the need to optimize the

energy efficiency management of ships and reduce greenhouse gas emissions through robust predictive models and the application of new technologies.

In the article “Modelling, Optimization, and Control of Ship Energy Systems Using Exergy Methods,” Trinklein et al. (2019) discuss the optimization of ship energy systems through exergy methods. They argue that by modelling multiple system domains simultaneously and applying the Second Law of Thermodynamics, it is possible to minimize total exergy destruction. This results in lower emissions and fuel costs, as well as more efficient, smaller, and lighter onboard systems.

In the study, “Operation-dependent exergetic sustainability assessment and environmental analysis on a large tanker ship utilizing Organic Rankine cycle system,” Morosuk and Tsatsaronis (2020) explore the assessment of exergy sustainability and environmental analysis dependent on the operation of a large tanker ship using an Organic Rankine Cycle (ORC) system. The study concludes that implementing the ORC can significantly improve energy efficiency and reduce environmental emissions of large tanker ships, highlighting the importance of exergy analysis to optimize operational sustainability and reduce environmental impacts.

Aijjou et al. (2020), in “Analysis of Container Ship Energy Systems,” explore the energy efficiency of medium-sized container ships. The analysis revealed that more than 80% of total energy consumption is caused by the propulsion plant, while electrical energy generation accounts for 14-17%. About 60% of the supplied energy is lost to the environment through the cooling system, radiation, friction, and exhaust from diesel engines. Exergy losses caused by exhaust gases and heat transfer are other significant contributors.

In the study “Thermodynamic and exergoeconomic analyses and optimization

of an auxiliary tri-generation system for a ship utilizing exhaust gases from its engine,” Morosuk and Tsatsaronis (2020) discuss the thermodynamic and exergoeconomic analysis of an auxiliary tri-generation system for ships utilizing exhaust gases from the engine. The study demonstrates that applying exergy and exergoeconomic analyses can identify opportunities for economic and energy optimization in onboard auxiliary systems, highlighting the importance of waste heat recovery to improve overall system efficiency.

Tran (2019), in the study “Investigate the energy efficiency operation model for bulk carriers based on Simulink/Matlab,” presents a numerical model for calculating the Energy Efficiency Operational Indicator (EEOI) considering environmental navigation conditions. This work highlights the need to optimize the energy efficiency management of ships and reduce greenhouse gas emissions through robust predictive models and the application of new technologies. The research used operational data from bulk carriers to validate the model and demonstrate how optimizing the main engine speed can save energy onboard and reduce greenhouse gas emissions.

In the article “Energy, Exergy and Environmental Analysis of ORC Waste Heat Recovery from Container Ship Exhaust Gases Based on Voyage Cycle,” Lyu et al. (2023) discuss waste heat recovery from container ship exhaust gases using the Organic Rankine Cycle (ORC). The study evaluates the energy, exergy, and environmental performance of an ORC system with different working fluids during a voyage cycle. The results indicate that Cyclohexane can generate the highest net power, while Benzene is more suitable for thermal efficiency. The exergy analysis identified the main components of the ORC system that need optimization, such as the evaporator and condenser.

These studies highlight the importance of energy and exergy analyses in identifying inefficiencies and optimization opportunities in ship energy systems. Applying these methodologies can lead to a significant reduction in CO₂ emissions and improvement in the energy efficiency of ships, aligning with current and future environmental regulations.

SPECIFIC GAPS IN CURRENT LITERATURE

The current literature emphasizes the importance of exergy analysis to identify energy inefficiencies in ships and the potential of exergy-based methodologies to optimize energy efficiency and reduce CO₂ emissions. However, there is a significant gap in applying these methodologies to select specific emission reduction technologies for different types of ships, especially considering their operational and maintenance peculiarities. While thermodynamic modelling is widely applied in container ships, bulk carriers, and tankers, the analysis in dynamically positioned Class 2 tankers, which require processes that do not compromise the vessel's redundancy and reliability, is still underexplored.

The objective of this study is not to develop new technology but to apply a new utility to energy and exergy modelling for a purpose distinct from those addressed in other studies. We propose identifying the ideal technologies for a specific ship and project, considering its design, maintenance, and operation specifics. In this way, we aim not only to reduce the vessel's emissions, but also to ensure that it meets the requirements of the IMO's Energy Efficiency Existing Ship Index (EEXI).

This approach aims to fill a specific gap in the current literature, which predominantly focuses on developing new technologies without adequately exploring the application of existing methodologies for the optimized selection of technologies in varied and specific

contexts of vessel operation. By offering a new application for energy and exergy modeling, this study provides a practical tool for selecting technologies that maximize energy efficiency and minimize CO₂ emissions in different types of ships, considering their operational and maintenance peculiarities.

THE STRUCTURE OF THIS ARTICLE IS AS FOLLOWS:

In Section 2, an exposition on the prominence of energy efficiency indicators set by the International Maritime Organization (IMO), notably the EEXI, is provided. This outline encompasses a detailed elucidation on how these indicators are computed, which compliance criteria are stipulated, and the overarching purpose of such regulations. In Section 3, the relationship between exergy and energy efficiency is described, revealing itself as a tool for assessing energy quality and process efficiency. Within the context of a vessel's energy efficiency, exergy analysis emerges as a method pinpointing inefficiencies, losses, and areas where energy quality is compromised. This directly correlates with efficiency indicators set by the IMO.

In Section 4, the guiding objectives of the study are elucidated, while in Section 5, a robust conceptual foundation is offered, addressing the core principles of energy and exergy.

In Section 6, a detailed data collection procedure is outlined, spanning two distinct operational stages of the main engine: during sea trial and after 10 years of operation. Additionally, a thermodynamic model representing the engine's energy performance at each of these stages is crafted.

Section 7, titled "Methods and Experience", entails exergy calculations for each of the engine's operational stages. This process affords a meticulous understanding of inefficiencies and losses that transpire over time. Furthermore,

at this juncture, the calculation of IMO-mandated energy efficiency indicators, like EEXI, for each stage is undertaken.

In Section 8, results from the exergy analysis are juxtaposed against IMO's energy efficiency indicator values for each stage. This scrutiny permits discerning how shifts in energy efficiency, as gauged by exergy, correlate with EEXI values, yielding invaluable insights into strategies for enhancing efficiency.

In Section 9, recommendations are formulated, and based on the comparative analysis undertaken, suggestions concerning operational practices or technological upgrades with the potential to boost the vessel's energy efficiency are presented, always bearing in mind the requirements imposed by the IMO.

In Section 10, titled "Results and Discussion – Case Study Conclusion," a thorough assessment is conducted to examine the impact of integrating a more efficient turbocharger and implementing heat recovery boilers, which produce steam for a turbogenerator, on the vessel's Attained Energy Efficiency Indicator (*EEXI_{att}*).

In Section 11, "Validation of Contribution to the Overall Vessel Efficiency," the results and conclusions are contextualized and validated through comparisons with pertinent literature, emphasizing the alignment of this study's findings with standards and estimates set by renowned researchers in the field.

In Section 12, the conclusions drawn from the study are summarized, consolidating the main discoveries and underscoring the significance of the findings in the realm of energy efficiency in vessels.

UNDERSTANDING IMO INDICATORS

ENERGY EFFICIENCY INDEX OF EXISTING SHIPS (EEXI)

GENERAL

The Existing Ship Energy Efficiency Index (EEXI) has been established as a prominent metric for assessing the energy performance of vessels. (Tran et al., 2019) taking to account that indicator provides a quantitative assessment of a ship's efficiency relative to pre-established benchmark parameters.

As highlighted by (Armstrong, V. et al., 2015), the primary objective of this metric is to encourage shipowners, operators, and crews to pursue more efficient practices and technologies, fostering continuous improvement in the maritime sector's energy efficiency.

The meticulous computation of the EEXI is structured in three fundamental stages. The first, as detailed by (Kontovas et al., 2013), involves the determination of the calculated EEXI. This phase demands a comprehensive analysis of various ship parameters, ranging from its architectural design to auxiliary and propulsion systems.

Subsequently, (Zhang, S. et al., 2019; Lindstad, H., 2015) emphasize the significance of the second stage, which centers on verifying the reduction factor. This step assesses whether the previously calculated EEXI aligns with the established regulatory standards. Within this framework, attributes like the ship's construction year and criteria set through the MEPC 334 resolution by the International Maritime Organization (IMO, 2021) come into play.

Concluding the process, (Anink et al., 2011) underscore the importance of determining the required EEXI in the third stage. This value, grounded in the IMO's guidelines concerning energy efficiency and CO₂ emission reduction

targets, is pivotal in guiding strategic decisions in the maritime sector, spanning design, operations, and future investments.

EEXI ATTAINED (EEXI_{att})

The Attained Energy Efficiency Existing Ship Index (*EEXI_{att}*) is the objective function representing the value of the ship's existing energy efficiency index attained by the vessel, based on decision variables and the thermodynamic constraints of the propulsion and generation system. It provides a realistic assessment of the vessel's energy efficiency performance, considering various factors such as its design, operational characteristics, and fuel consumption data.

The attained EEXI (*EEXI_{att}*) is calculated using Equation 1, and the result is compared to the required EEXI of the vessel.

EEXI REQUIRED (EEXI_r)

The required EEXI represents the target value for energy efficiency that ships must achieve. It is based on a reference value, adjusted by an applicable reduction factor. This reference value is determined based on the standard operational characteristics of ships, while the reduction factor (*F red*) is defined by the IMO, considering the type and size in Marpol Convention, Annex6 chapter 4.

The determination of the required EEXI considers the energy efficiency of similar ships, thereby setting a standard that existing ships should strive to meet or exceed.

The required EEXI (*EEXI req*) is calculated using the following formula:

$$EEXI req = EEXI ref \times (1 - F red) \quad (1)$$

Where:

- *EEXI reference (EEXI ref)* the baseline value set by the IMO for a specific type and size of ship. (IMO, 2022)

- *F reduction factor (F red)* is determined by the IMO and can vary based on the type and size of the ship. (IMO, 2022)

CORRELATION BETWEEN OBTAINED EEXI, REQUIRED EEXI AND REDUCTION FACTOR

To meet energy efficiency targets set by the Maritime Organization International (IMO), it is ideal that the energy efficiency indicator obtained for a ship is lower than required

According to MARPOL 6, Chapter 4, Rule 21, the EEXI value achieved must be lower than the required, as indicated by Equation 3.

Equation 2 specifies that the EEXI attained must exceed the EEXI required. This one calculation and comparative approach are used to enforce the measures IMO regulations (IMO (2022). MEPC.333(78)) on the energy efficiency of ships to reduce greenhouse gas emissions and promote more sustainable practices in the maritime industry.

$$EEXI attained (EEXI_{att}) \leq EEXI required (EEXI_{req}) \quad (2)$$

If a ship fails to meet regulatory requirements, it is imperative to explore ways to invest in processes and/or innovative technologies that effectively mitigate CO₂ emissions.

Script:

EEXI - energy efficiency existing ship index (gCO₂/Ton.mile)

SFC - specific fuel consumption (g/kWh).

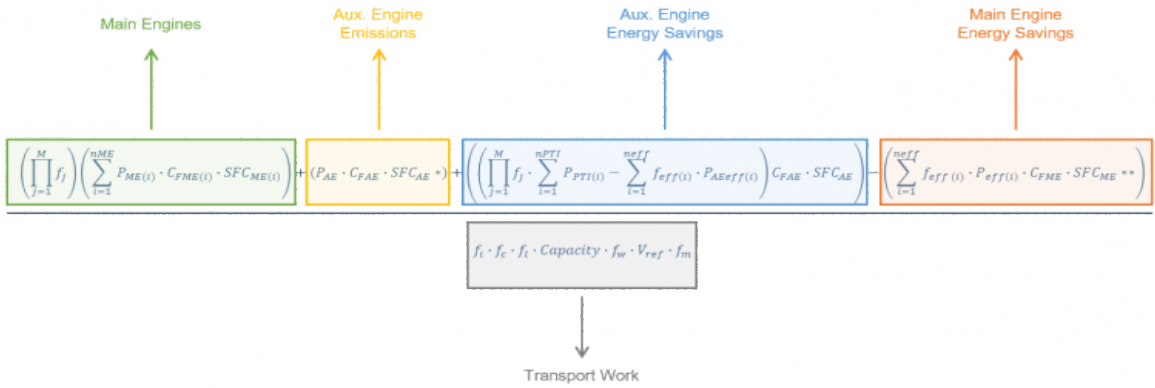
Cf - carbon emission factor (tCO₂/t fuel)

P - power (W).

DWT - deadweight (tonnage).

V - speed (knot).

f - correction factors.



Formula 3: EEXI formula achieved.

Subscript:

- att - attained.
- ME - main engine.
- AE - auxiliary engine.
- ref - reference.
- eff - innovative technology.
- j - specific vessel design elements.
- PTI - power Take In (provides temporary extra power to the main engine propulsion system).
- i- factor for technical/regulatory limitation on capacity
- c - cubic capacity correction
- w - Factor for speed reduction at sea
- m - correction factor for ice-class ships

RELATIONSHIP BETWEEN EXERGY AND ENERGY EFFICIENCY

Thermodynamic modeling, as per (Frangopoulos, C.A., 2018; Deniz, C., 2015), through exergy analysis, constitutes a valuable analytical tool that significantly contributes to understanding the thermodynamic constraints inherent in a design, as well as pinpointing inefficiencies in energy use. Through this approach, it is possible to effectively map out the energy distribution

in a vessel’s main engine, pinpointing where energy wastage occurs.

Once we understand the energy allocation in this context and accurately identify areas of waste, it becomes feasible to direct optimization efforts to the exact spots where energy improvements are needed. This approach not only ensures compliance with established energy efficiency indicators, such as those promulgated by the International Maritime Organization (IMO), but also results in tangible interventions that enhance the vessel’s sustainability.

Optimizing the vessel’s propulsion system, based on exergy analysis, goes beyond merely seeking regulatory compliance. It embraces a genuine commitment to sustainability by directing resources and efforts to critical areas where improvements in energy efficiency can translate into significant reductions in energy consumption and, consequently, greenhouse gas emissions. This approach not only aligns the vessel with increasingly stringent environmental regulations but also makes a substantial contribution to preserving the marine environment and mitigating climate change.

The issue at hand is to achieve the lowest possible EEXI value, which represents CO₂ emissions per nautical mile, where thermodynamic constraints are tied to the specific heat of the fuel used and energy

wastage, which can be identified through thermodynamic modeling and the subsequent exergy analysis of the system.

OBJECTIVE FUNCTION, DECISION VARIABLES, AND THERMODYNAMIC CONSTRAINTS

The EEXI (Energy Efficiency Existing Ship Index) is an operational indicator proposed by the IMO to assess the energy efficiency of existing vessels. It is calculated based on the ship's energy consumption in relation to its transport capacity.

In the formulation of the EEXI, the factors that can be characterized as decision variables are those that can be adjusted or controlled to enhance the vessel's energy efficiency, such as innovative averages applied to the energy generation system or propulsion or even fuel alteration.

According to (Reini et al., 2020), the optimization is subject to a thermodynamic constraint to factors such as energy balance. Those which can be characterized as thermodynamic constraints are those that impose physical and thermodynamic limitations on the vessel's energy efficiency. These constraints may include, for instance:

- **Energy Conservation:** The vessel must adhere to the law of energy conservation, meaning the consumed energy should equal the supplied energy minus the losses. This imposes a thermodynamic constraint on the vessel's energy consumption.
- **Engine Efficiency:** The vessel's engine has a maximum efficiency, which imposes a thermodynamic constraint on energy consumption. Engine efficiency can be influenced by factors like operating temperature, operating pressure, and fuel efficiency.

- **Design Constraints:** The vessel may have design constraints that affect its energy efficiency, such as hull shape, forward resistance, propulsion system efficiency, among others.

In the realm of maritime engineering and naval architecture, the performance of a ship's engine is inherently interconnected with its propulsive efficiency, which in turn plays a crucial role in the overall performance of the vessel. The intricate relationship between these parameters can be understood through a systemic approach that examines the interactions between the engine's output and the hydrodynamic characteristics of the ship.

The central premise holds that enhancements in engine performance, typically measured by parameters such as power output, fuel efficiency, and emissions, have a direct and proportional impact on the ship's propulsive efficiency. This propulsive efficiency pertains to the ship's capability to convert engine power into thrust, effectively overcoming resistive forces such as water and air resistance to navigate through the marine environment.

Improvements in engine technology, such as advanced combustion techniques, turbocharging, and exhaust gas recirculation, can lead to higher thermal efficiency, resulting in more energy being transformed into useful work. This improvement in engine performance usually translates into greater thrust for propulsion, provided that the propeller and hull designs are optimized to capitalize on the increased power. Consequently, a more powerful and efficient engine can enhance the ship's speed and reduce the Specific Fuel Oil Consumption (SFOC), thus improving the operational efficiency and environmental sustainability of the vessel.

To harmonize these advancements, the concept of ship efficiency must be approached holistically, considering not just the propulsion machinery, but also the

interaction between the hull form, surface condition, propeller choice and condition, and the vessel's operational practices. The overall efficiency of a ship is often assessed by the Energy Efficiency Design Index (EEDI) and Energy Efficiency Existing Ship (EEXI), which considers propulsive performance and engine efficiency as parts of a larger equation aimed at reducing environmental impact and increasing energy efficiency in maritime transport.

INTERTEMPORAL OPTIMIZATION

(Frangopoulos, C.A., 2018), defined intertemporal optimization as the optimization that takes into account the various operational conditions a system encounters over its lifespan and determines the operational state at each moment in time that results in the overall minimum or maximum of the objective function.

Intertemporal optimization of systems modeled using thermodynamics refers to the maximization of an objective function over time, considering the thermodynamic constraints of the system. These constraints might include thermodynamic limitations such as energy conservation, mass conservation, and thermodynamic equilibrium constraints.

PURPOSE OF THE STUDY

The central question posed is: "Why optimization?" As prudent energy resource management and environmental protection become increasingly pressing imperatives, it is often perceived that these objectives may compete. Simply seeking improvement is no longer sufficient; what is required is optimization, that is, achieving the best outcome under specific circumstances.

The intertemporal optimization of integrated energy systems on vessels emerges as a critical endeavor. Energetic and exergetic modeling presents itself as an indispensable tool for

the analysis and optimization of these energy systems. Its primary objective is to identify technologies that can effectively maximize a vessel's energy use, thereby contributing to meeting the criteria of the Energy Efficiency Existing Ship Index (EEXI).

The main goal of this study is to develop a methodology based on the practical application of thermodynamic principles to address the issue of adequacy in existing vessels that are not in line with the Energy Efficiency Index established and approved by the IMO. This paper aims to identify, through this methodology, more effective and assertive ways to meet these standards and, consequently, reduce emissions.

This methodological approach entails a thorough analysis of the vessel's energy and exergy efficiency, enabling the identification of parameters in the EEXI formula 1 that can be effectively implemented in practice. These parameters are intrinsically linked to systems meticulously outlined by energy and exergy analyses, which empower us to discern weaknesses and energy dissipation. From this identification, it becomes possible to select the most appropriate innovative technologies to enhance the vessel's energy efficiency.

The scientific contribution to the naval field lies in demonstrating the application of existing theoretical concepts in addressing practical challenges related to energy efficiency and in providing tangible solutions to real-world challenges in the maritime industry. This contribution, therefore, promotes the advancement of maritime engineering, aids in mitigating pollutant emissions, and plays a pivotal role in guiding technical decision-making in a multifaceted context.

FUNDAMENTALS OF EXERGY

Exergy in a system is defined as the maximum work that can be performed by a system as it interacts with its external environment. It can be mathematically expressed in a general form, as shown in Equation 4. (Pierre et al., 2016)

$$E = Q - T_o \cdot (S - S_o) \quad (4)$$

Script:

E - Exergy

Q - Heat

S - Entropy

T - Temperature

Subscript:

o - Environment

Exergy analysis is closely related to the notion of energy quality in a thermodynamic process applied to a control volume. Mathematically, exergy analysis can be described in a specific manner, as shown in Equation 5. (Marty, 2016).

$$E = (U - U_o) + P_o(V - V_o) - T_o(S - S_o) \quad (5)$$

Script:

E - Exergy

W - Work

Q - Heat

U - Internal energy.

P - Pressure

V - Volume

T - Temperature

S - Entropy

Subscript:

o - Environment

In this article, it was considered, as well as by (Sondermann, C, 2013), in the exergy balances of engines, that kinetic and potential energy, as well as other forms of energy such as chemical and electrical energy, are insignificant.

Exergy analysis plays a pivotal role in assessing the energy efficiency of a system and pinpointing areas where improvements can be implemented to minimize energy losses and maximize the potential for useful work.

Exergy considers not only the amount of energy, but also its quality and its ability to be efficiently converted into work.

Considering the ambient temperature, the available exergy can be assessed. It refers to the amount of energy that can be effectively converted into useful work in the specific operating environment of the system.

DIAGRAM OF GRASSMANN

The Grassmann diagram is a graphical representation that visualizes the interconnections between the components and the exergy losses in a ship's energy system. Its purpose is to identify specific areas where improvements can be implemented to increase energy efficiency and reduce exergy losses.

This diagram serves as a valuable tool for optimizing ship energy systems and promoting more efficient and sustainable operations.

This diagram has a format similar as demonstrated in figure 1.

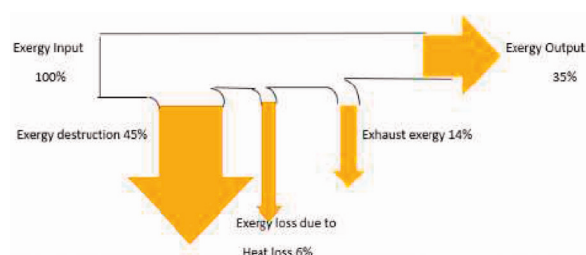


Figure 1: Energy distribution scheme using Grassmann diagram. (Source: Panigrahi,, 2018) [19]

DATA COLLECTION AND MODELLING

Data collection and information gathering employed an in situ procedure within the real operational environment of a 23-year-old oil tanker equipped with a Hyundai B&W 6S60MC-6 engine, operating in Brazilian waters from May 21 to June 15, 2022.

Throughout the specified periods, a series of measurements and observations were made on board the vessels to deeply understand their energy and operational performance. This encompassed collecting data related to fuel consumption and the operational characteristics of the main engines, as well as gathering data during different stages of the main engine's operation: sea trial and after 23 years of operation.

General information about the vessel was also obtained as shown in Table 1, as well as environmental conditions such as water temperature, ambient engine room temperature, and meteorological conditions as depicted in Table 2.

Ship Type	DWT	Overall Length	Beam	Year	Main Engine
Tanker	153,117 tons	273.95m	50m	1999	Hyundai B&W 6S60MC-6

Table 1: Main Characteristics of the Vessel

(Source: Vessel Description Document)

Script

DWT – Deadweight Tonnage

The data collection measures involved the use of specialized instrumentation, such as pressure sensors, fuel flow meters, thermometers, and exhaust gas monitoring equipment, all integrated into the lines and systems. In addition, interviews and interactions with the onboard crew were conducted to obtain additional contextual information and clarifications about operational procedures.

Period	Average Temperature During Period	General Environmental Conditions During Period
1998 / 2022	°C	Escala Beaufort (grade)
December 1 to 10, 1998	15	variable among 1 at 3
May 21 to June 15, 2022	33	variable among 1 at 4

Table 2: Data Collection Period and Environmental Conditions

(Source: Sea Trial Report and Author)

In this article, the average temperature of the environment and seawater was considered the same.

The collection of sea trial information considered the sea trial report, where information was obtained for the period from December 1st to 10th, 1998.

ACQUISITION AND VALIDATION OF INPUT DATA

For the acquisition of thermodynamic properties, this study employed the NIST Reference Fluid Thermodynamic and Transport Properties Database (REFPROP) along with the Thermonator software. These tools are integral in providing accurate and reliable data essential for the analysis of thermodynamic systems and to validation used to Python.

METHODS AND EXPERIENCE

The methodology for analysis and optimization of energy systems represents a holistic and integrated approach, grounded in the principles of thermodynamics and optimization, aiming to enhance energy efficiency and, consequently, contribute to mitigating the energy and environmental challenges faced in various areas of engineering and industry.

In the methodological process outlined here, four crucial phases are distinguished, which are intrinsically linked to the analysis

and optimization of energy systems. Each of these stages plays a vital role in the systematic approach adopted to enhance energy efficiency. The stages will be detailed further as follows:

Stage 1. Energy System Modeling Using Thermodynamics: This inaugural stage involves creating an energy system model based on the principles and laws of thermodynamics. This procedure encompasses the detailed identification and description of system components, such as equipment, processes, and energy flows. Additionally, at this stage, the set of thermodynamic equations detailing the system's behavior is formulated. This thermodynamic modeling serves as the conceptual and mathematical foundation upon which all subsequent analysis relies.

Stage 2. Exergy Waste Identification: Exergy, representing the measure of the energy quality available for performing useful work, is the central focus of this stage. Here, a thorough exergetic analysis is conducted to pinpoint exergy losses occurring in the system. This exergetic analysis process involves evaluating the irreversibility and inefficiencies inherent in the system's processes and equipment, resulting in exergy waste. Such an analysis provides a comprehensive insight into critical areas where energy efficiency can be enhanced.

Stage 3. System Optimization Through the EEXIatt Objective Function: The third stage of this methodology adopts an optimization approach to maximize the system's energy efficiency. To achieve this, the EEXIatt (Energy Efficiency Existing Ship Index) objective function, an indicator proposed by the International Maritime Organization (IMO), is used to assess the energy efficiency of existing ships. Here, the decision variables and thermodynamic constraints obtained from the exergetic analysis are incorporated into the objective function formulation, thus outlining the optimization problem.

The ultimate goal is to find the system configuration and operation that minimizes the EEXIatt, i.e., maximizes energy efficiency, as per the standards set by the IMO.

Stage 4. Corrective Action and Improvement Identification: Finally, based on the results obtained in the optimization stage and the previous exergetic analysis, corrective actions and improvements are identified. These measures aim to reduce exergy waste and consequently enhance the system's overall energy efficiency. Corrective actions may include equipment modifications, process optimizations, the implementation of more efficient technologies, and other relevant strategies. The primary purpose of these actions is to minimize exergy losses and maximize energy's efficient use, promoting sustainability and meeting regulatory norms.

To demonstrate the methodology, we present its implementation in a case study conducted on the Hyundai B&W 6S60MC-6 engine of an oil tanker, as shown in Table 1.

EXERGY EFFICIENCY CALCULATIONS

To perform an energy efficiency analysis of the Hyundai B&W 6S60MC-6 engine, several parameters and factors must be considered.

These parameters are outlined in Table 3, which includes power, thermal efficiency, specific fuel oil consumption (SFOC), mass, enthalpies, and entropy of the air, Fresh water jacket cooler (FWJC), and engine exhaust gases.

Through of measured values and analyzing these variations, it becomes possible to evaluate the efficiency of the engine's energy conversion and identify potential areas of improvement.

MODELLING DESCRIPTION

The analysis focuses on evaluating engine performance through a series of thermodynamic and mechanical calculations. This involves converting power units, calculating specific fuel consumption, fuel consumption, and total heat generation. These calculations are essential for understanding the engine's efficiency and energy output over different years. By converting power to kW and evaluating specific fuel consumption in both 1998 and 2022, the study aims to compare the operational efficiency and fuel utilization of the engine.

Furthermore, the study includes a detailed assessment of cooling water and exhaust gas parameters to analyze.

CONVERSION OF POWER TO kW

Power is often converted to kW for easier comparisons and calculations. Below, we perform the conversion of common power units to kW:

PS to kW:

$$1 \text{ PS is equal to } 0.7355 \text{ kW. (6)}$$

BHP to kW:

$$\text{BHP} = 12100 \times 0.7355 \approx 8899.55 \text{ kW (7)}$$

IHP to kW:

$$\text{IHP} = 12801 \times 0.7355 \approx 9410.60 \text{ kW (8)}$$

CONVERSION OF SPECIFIC FUEL CONSUMPTION

Specific fuel consumption is a measure of how efficiently an engine converts fuel into mechanical energy. The conversion is presented below:

1998:

$$\text{Specific Fuel Consumption (SFC)} = 167.81 \text{ g/kWh} = 0.16781 \text{ kg/kWh (9)}$$

2022:

$$\text{Specific Fuel Consumption (SFC)} = 179 \text{ g/kWh} = 0.179 \text{ kg/kWh (10)}$$

CALCULATION OF FUEL CONSUMPTION

Fuel consumption is calculated by multiplying the engine power by the specific fuel consumption:

1998:

$$\text{Fuel Consumption} = \text{BHP} \times \text{SFC} = 8899.55 \text{ kW} \times 0.16781 \text{ kg/kWh} \approx 1493.28 \text{ kg/h (11)}$$

2022:

$$\text{Fuel Consumption} = \text{BHP} \times \text{SFC} = 8899.55 \text{ kW} \times 0.179 \text{ kg/kWh} \approx 1593.02 \text{ kg/h (12)}$$

CALCULATION OF TOTAL HEAT

The total heat generated by the engine is determined by the fuel consumption multiplied by the fuel's calorific value and converted to kW:

1998:

$$Q = \text{Fuel Consumption} \times \text{Fuel Calorific Value} \times (1 \text{ kWh} / 3.6 \text{ MJ})$$

$$Q = 1493.28 \text{ kg/h} \times 42.81 \text{ MJ/kg} \times (1 \text{ kWh} / 3.6 \text{ MJ}) \approx 17766.86 \text{ kW (13)}$$

2022:

$$Q = \text{Fuel Consumption} \times \text{Fuel Calorific Value} \times (1 \text{ kWh} / 3.6 \text{ MJ})$$

$$Q = 1593.02 \text{ kg/h} \times 42.81 \text{ MJ/kg} \times (1 \text{ kWh} / 3.6 \text{ MJ}) \approx 18936.36 \text{ kW (14)}$$

SHAFT EQUIVALENT HEAT (QBP)

Considering there is no change in power between the years, the shaft equivalent heat (Qbp) is equal to the BHP in both years:

1998 and 2022:

$$Q_{bp} = \text{BHP} = 8899.55 \text{ kW (15)}$$

COOLING WATER ANALYSIS

SPECIFIC HEAT CALCULATION

The specific heat of the cooling water is calculated as follows:

1998:

$$Q_{fwj} = \dot{m} \times c_p \times (T_s - T_e)$$

$$Q_{fwj} = 27 \text{ kg/s} \times 4.186 \text{ kJ/kg}^\circ\text{C} \times (349.15 - 343.15) \text{ K} \approx 678.18 \text{ kW} \quad (16)$$

2022:

$$Q_{fwj} = \dot{m} \times c_p \times (T_s - T_e)$$

$$Q_{fwj} = 27 \text{ kg/s} \times 4.186 \text{ kJ/kg}^\circ\text{C} \times (358.15 - 347.15) \text{ K} \approx 1230.14 \text{ kW} \quad (17)$$

SPECIFIC EXERGY OF WATER

The specific exergy of water represents the maximum useful work that can be obtained from the cooling heat:

1998:

$$\text{Specific Exergy} = c_p \times ((T_s - T_e) - T_{amb} \times \ln(T_e / T_s))$$

$$\text{Specific Exergy} = 4.186 \times ((349.15 - 343.15) - 287.65 \times \ln(343.15 / 349.15)) \approx 5.40 \text{ kJ/kg} \quad (18)$$

2022:

$$\text{Specific Exergy} = c_p \times ((T_s - T_e) - T_{amb} \times \ln(T_e / T_s))$$

$$\text{Specific Exergy} = 4.186 \times ((358.15 - 347.15) - 306.15 \times \ln(347.15 / 358.15)) \approx 10.55 \text{ kJ/kg} \quad (19)$$

TOTAL EXERGY OF WATER

The total exergy of the cooling water is calculated by multiplying the mass flow rate by the specific exergy:

1998:

$$\text{Total Exergy} = \dot{m} \times \text{Specific Exergy} = 27 \text{ kg/s} \times 5.40 \text{ kJ/kg} \approx 145.80 \text{ kW} \quad (20)$$

2022:

$$\text{Total Exergy} = \dot{m} \times \text{Specific Exergy} = 27 \text{ kg/s} \times 10.55 \text{ kJ/kg} \approx 285.65 \text{ kW} \quad (21)$$

EXHAUST GAS HEAT CALCULATION

The heat of the exhaust gases is calculated by multiplying the mass flow rate by the specific heat capacity and the temperature difference between the inlet and outlet:

1998:

$$Q_{eg} = \dot{m} \times c_p \times (T_{gde} - T_{gds})$$

$$Q_{eg} = 3.11 \text{ kg/s} \times 1.1 \text{ kJ/kg}^\circ\text{C} \times (621.15 - 489.15) \text{ K} \approx 450.70 \text{ kW} \quad (22)$$

2022:

$$Q_{eg} = \dot{m} \times c_p \times (T_{gde} - T_{gds})$$

$$Q_{eg} = 3.11 \text{ kg/s} \times 1.1 \text{ kJ/kg}^\circ\text{C} \times (723.15 - 489.15) \text{ K} \approx 800.73 \text{ kW} \quad (23)$$

SPECIFIC EXERGY OF GASES

The specific exergy of the exhaust gases is calculated, considering the ability to convert the heat of the gases into useful work:

1998:

$$\text{Specific Exergy} = c_p \times ((T_{gde} - T_{gds}) - T_{amb} \times \ln(T_{gds} / T_{gde}))$$

$$\text{Specific Exergy} = 1.1 \times ((621.15 - 489.15) - 287.65 \times \ln(489.15 / 621.15)) \approx 97.16 \text{ kJ/kg} \quad (24)$$

2022:

$$\text{Specific Exergy} = c_p \times ((T_{gde} - T_{gds}) - T_{amb} \times \ln(T_{gds} / T_{gde}))$$

$$\text{Specific Exergy} = 1.1 \times ((723.15 - 489.15) - 306.15 \times \ln(489.15 / 723.15)) \approx 134.90 \text{ kJ/kg} \quad (25)$$

TOTAL EXERGY OF GASES

The total exergy of the exhaust gases is obtained by multiplying the mass flow rate by the specific exergy:

1998:

$$\text{Total Exergy} = \dot{m} \times \text{Specific Exergy} = 3.11 \text{ kg/s} \times 97.16 \text{ kJ/kg} \approx 302.19 \text{ kW} \quad (26)$$

2022:

$$\text{Total Exergy} = \dot{m} \times \text{Specific Exergy} = 3.11 \text{ kg/s} \times 134.90 \text{ kJ/kg} \approx 419.54 \text{ kW} \quad (27)$$

ANALYSIS OF FRICTION LOSSES

Friction losses are calculated to evaluate the mechanical efficiency of the engine. The effective power (Qbp) is equal to the shaft power (bp):

1998 and 2022:

$$Q_{bp} = bp = 8899.55 \text{ kW} \quad (28)$$

FRICTION LOSSES

Friction losses, including mechanical losses, are determined by subtracting the effective power (bp) from the indicated power (ip):

1998:

$$\text{Losses (including friction)} = ip - bp = 9410.60 - 8899.55 \approx 511.05 \text{ kW} \quad (29)$$

2022:

$$\text{Losses (including friction)} = ip - bp = 9410.60 - 8899.55 \approx 511.05 \text{ kW} \quad (30)$$

These calculations are now adjusted with the corrected specific fuel consumption values for 1998 and 2022.

Parameter	Energy (kW) (1998)	Exergy (kW) (1998)	Exergy Loss (kW) (1998)	Energy (kW) (2022)	Exergy (kW) (2022)	Exergy Loss (kW) (2022)
Cooling Water	678.18	145.8	532.38	1230.14	285.65	944.49
Exhaust Gases	450.7	302.19	148.51	800.73	419.54	381.19
Indicated Power (ip)	9410.6	8899.55	511.05	9410.6	8899.55	511.05
Total Heat (Q)	13354.97	-	-	14168.29	-	-
Shaft Equivalent Heat (Qbp)	8899.55	8899.55	0	8899.55	8899.55	0

Table 3: Comparison of Engine Energy Balance in 1998 and 2022

(Source: Sea Trial Report and Author)

WORK SYSTEM MAPPING

The system mapping must be done considering the order of passage of the engine cooling water fluid through the equipment, which in this study were termed as markers.

Figure 2 illustrates the system flow mapping and the individual equipment components.

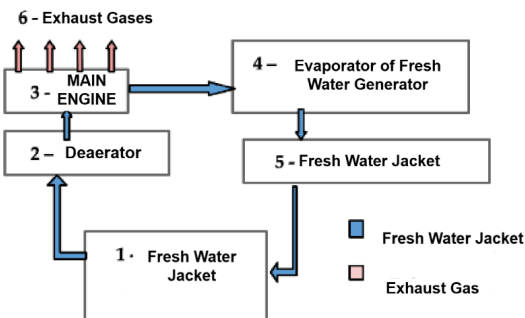


Figure 2: Flow Mapping of the System (Source: author)

In the system depicted in Figure 2, the freshwater jacket, responsible for cooling the main engine, follows a specific path. Initially, this water is directed to the distiller, where a distillation process takes place to eliminate impurities and undesirable substances from the water. In Table 4, it is possible to verify the temperatures and pressures measured in the system.

Equipment	In/ Outs	Temperature (°C) 1998	Temperature (°C) 2022	Pressure (bar) 1998	Pressure (bar) 2022
Fresh water jacket Pump	in	65,00	70,00	1.15	3.55
	out	65.8	76,00	4,55	3.55
Deaerator	in	65.8	76,00	4,55	3.55
	out	70,00	74,00	4,55	3.55
Main Engine	in	70,00	74,00	3,00	3.55
	out	80,00	85,00	3,00	3.55
Distillation System	in	78,00	85,00	3,00	3,00
	out	70,00	70,00	2.78	2.78
Fresh water jacket cooler	in	68,00	70,00	3,00	3,00
	out	65,00	65,00	2.78	2.78

Table 4: Temperatures and Pressures of the system (Source: author)

After passing through the distiller, the water flow is directed to the cooler. In this stage, the water is cooled, typically by a heat exchanger, to regulate its temperature before proceeding to the subsequent phases of the system.

Subsequently, the water goes through the deaerator. This step aims to remove dissolved air from the water, as the presence of air can lead to operational complications and impact the overall efficiency of the system.

Finally, the treated water returns to the propulsion engine, where it acts as jacket water, actively involved in cooling the main engine. This water plays a crucial role in controlling the engine's temperature, ensuring optimal performance and efficiency.

This continuous water flow, encompassing the freshwater generator, cooler, deaerator, and subsequent return to the propulsion engine, constitutes a cycle of water treatment and recirculation of jacket water. This cycle ensures the quality and effectiveness of the main engine cooling system of the installation.

EXERGY EFFICIENCY ANALYSIS

In the exergy analysis of the system, the primary emphasis is placed on the work and heat generated in the engine. Factors such as kinetic energy and potential energy are deemed negligible in this analysis. By focusing on work and heat, a more precise evaluation of the exergy distribution in the system can be achieved.

Table 5 displays the exergy analysis and energy loss of the Hyundai B&W 6S60MC-6 engine operating in an environment of 15°C (Sea Trial – 1998), and Table 6 shows the engine operating in a 33 °C environment in 2021. Exergy and energy loss are closely intertwined in a system. Both tables show the values obtained from the equations of exergy balance in Appendix 2.

Exergy represents the portion of the system's energy with the potential to be converted into useful work, considering environmental conditions. On the other hand, energy loss refers to the portion of energy that cannot be converted into useful work. The exergy and energy loss analysis provides valuable insights into the engine's energy efficiency and utilization.

Exergy	Energy use	Exergy loss
Ebp - Shaft Exergy	66.64%	-
Efwjc - Fresh Water Jacket Cooler	6.50%	3.02%
Eeg - Exhaust Gases Exergy	4.23%	2.22%
Epd - Losses Exergy	-	27.02%
Total	77.37%	32.26%

Table 5: Engine operating in a 15° environment
(Sea test - 1998)
(Source: author)

Energy loss refers to the portion of energy that cannot be used to perform useful work, being dissipated as heat, friction, leaks, and other types of losses. Exergy analysis plays a crucial role in identifying and quantifying these energy losses, offering a comprehensive understanding of the inefficiencies and areas that can be enhanced in a system.

In fact, the relationship between exergy and energy loss allows for an assessment of a system's energy efficiency. A smaller energy loss proportionally to the total exergy indicates a higher level of efficiency in using the available energy to perform useful work.

In calculating exergy, the ambient temperature is indeed a crucial factor. In this case, the ambient temperature is 33 °C. The ambient temperature and seawater temperature were adopted as the same temperature. This value provides a realistic estimate for the exergy analysis.

Exergy	Energy Use (%)	Exergy Loss (%)
Ebp - Shaft Exergy	62.81%	-
Efwjc - Fresh Water Jacket Cooler	6.50%	3.02%
Eeg - Exhaust Gases Exergy	4.23%	2.22%
Epd - Losses Exergy	-	27.02%
Total	77.37%	32.26%

Table 6: Engine operating in a 33° environment (Current situation — 2022)

Source: author

In a comprehensive academic analysis on the exergetic performance of maritime engine systems under different environmental conditions, efficiencies for the years 1998 (ambient temperature of 15°C) and 2022 (ambient temperature of 33°C) were examined. The analysis considered different components and their exergetic contributions.

In 1998, the exergy of the heat associated with shaft losses (Ebp) stood at 66.64%. However, in 2022, there was a reduction to 62.81%, suggesting a decrease in efficiency in extracting exergy from the engine shaft. In contrast, the exergy associated with engine cooling water (Efwjc) showed a significant increase from 1.09% in 1998 to 6.50% in 2022. The exergy from exhaust gases heat (Eeg) demonstrated a slight reduction from 2.26% in 1998 to 4.23% in 2022. The friction components (Ea) and losses (Epd), being loss-related, do not bring any direct contribution to the total exergy in both analyzed years.

When observing the exergetic losses, it's evident that the shaft losses (Ebp) remained stable in both years. However, there was a considerable increase in exergetic losses associated with engine cooling water (Efwjc) from 3.99% in 1998 to **3.02%** in 2022. Conversely, exergetic losses from exhaust gases (Eeg) showed a decrease from 1.11% in 1998 to 2.22% in 2022. Exergetic losses due to friction (Ea) slightly decreased from **30.01%** in 1998 to 27.02% in 2022, while

exergetic losses associated with other losses (Epd) had an increase from 35.11% in 1998 to 32.26% in 2022.

Table 07 presents the values of lost exergy, which allow quantifying the exergy losses in the system. By identifying the critical points where the most significant losses occur, it becomes possible to focus optimization and improvement efforts on these specific areas. This approach enables a more efficient allocation of resources and maximization of exergy in the system.

The comprehensive data pertaining to the engine specifications and performance metrics are meticulously cataloged in Appendix 1. This repository includes all relevant numerical values, operational parameters, and performance characteristics necessary for a thorough evaluation of the engine's capabilities within the context of this study.

Furthermore, the theoretical framework and mathematical formulations employed for the calculation of exergetic efficiency, applied in Table 7, are extensively delineated in Appendix 2. This section encompasses the derived equations, boundary conditions, and assumptions that underpin the exergetic analysis. The methodologies outlined herein adhere to the principles of thermodynamics and are crucial for the subsequent interpretation of the engine's energy efficiency from an exergy perspective.

Exergy Loss	Engine Operating (Sea Trial - 1998)	Engine (Current Situation - 2022)
Efwjc - Fresh Water Jacket Cooler	3.99%	3.02%
Eeg - Exhaust Gases Exergy	1.11%	2.22%
Epd - Losses Exergy	30.01%	27.02%
Total	35.11%	32.26%

Table 7: Comparative table of lost exergy in the years 1998 and 2022

source: author

In Table 07, in 1998, the exergetic loss associated with the engine cooling water (Efwjc) was recorded at 3.99%. However, in 2022, this loss decreased to 3.02%. Regarding the exergy of the exhaust gases (Eeg), there was a slight increase in exergetic losses from 1.11% in 1998 to 2.22% in 2022. As for other losses (Epd), there was a reduction in exergetic losses, going from 30.01% in 1998 to 27.02% in 2022.

With this data in hand, we see that in this system, the greatest benefit will come from the application of technology to harness the residual heat from the engine's exhaust gases.

DETAILED METHODOLOGY OF EXERGY ANALYSIS

The exergy analysis methodology aims to quantify the inefficiencies within the engine system by evaluating the destruction of exergy in various components. This approach provides a comprehensive understanding of the potential for improvement. The key steps involved in the exergy analysis are:

SELECTION OF SYSTEM BOUNDARIES:

Define the boundaries of the engine system to include the main engine, auxiliary systems, cooling water systems, and exhaust gas systems. The analysis focuses on the fuel system, cooling system, friction losses, atmospheric losses, and exhaust gases as key parameters.

Calculation of Exergy Destruction:

Use the first and second laws of thermodynamics to calculate the exergy destruction in each component. The exergy destruction is computed using the following general formula:

$$\text{Exergy destruction} = \text{Exergy input} - \text{Exergy output} \quad (31)$$

For each component, the specific exergy destruction is calculated by considering the inlet and outlet exergy values. Contour curves

for exergy analysis were used, considering only the fuel, cooling, friction losses, and exhaust gases as parameters.

APPLICATION TO SHIP SYSTEMS:

Apply the exergy destruction calculations to the engine's cooling water system (Efwjc), exhaust gas system (Eeg), and other loss mechanisms (Epd).

DERIVATION OF EXERGY EFFICIENCY METRICS:

Exergy efficiency (η_{exergy}) is derived by comparing the useful exergy output to the total exergy input. The efficiency metric is calculated using the formula:

$$\eta_{\text{exergy}} = \text{Total exergy input} / \text{Useful exergy output} \quad (32)$$

CONSIDERATION OF AVERAGE TEMPERATURE:

The average temperature for the period was extracted from the ship's Power Manager System, providing a realistic basis for the exergy analysis. The ambient temperature plays a crucial role in determining the exergy destruction and efficiency.

INTERPRETATION OF EXERGY ANALYSES RESULTS:

The derived exergy efficiency metrics are interpreted to identify areas with the highest exergy destruction, indicating potential for efficiency improvements. The analysis revealed that despite an apparent increase in available energy and exergy due to the higher temperature in 2022, there was a significant increase in exergy loss. This indicates that the ship is producing less output relative to its design capacity. Specifically, for the same projected power, the ship in 2022 is consuming more fuel and provide the same power as in 1998, making it comparatively inefficient in 2022.

GRASSMANN DIAGRAM OF THE SHIP

Using the results obtained in Table 5 and Table 6, the Grassmann diagrams can be derived. Figures 4 and 5 visually represent the relationships between the studied variables, providing a clear and intuitive view of the data. This graphical representation aids in analyzing and understanding the interactions between the variables, helping to identify patterns, trends, and significant correlations.

The Grassmann diagrams illustrate the flow of exergy through the various components of the engine system, highlighting where exergy is being utilized effectively and where it is being lost. These diagrams serve as a valuable tool for visualizing the efficiency of the engine's operation and identifying key areas for improvement.

In 1998 (Figure 4) and 2022 (Figure 5) show the exergy distribution and losses within the engine system, using data from Table 7: Comparative table of lost exergy in the years 1998 and 2022. The width of each flow represents the magnitude of exergy associated with each component. The diagrams are divided into sections that correspond to different parts of the engine system:

- **Shaft Exergy (Ebp):** Represents the useful work output of the engine.
- **Fresh Water Jacket Cooler Exergy (Efwjc):** Indicates the exergy lost through the engine cooling system.
- **Exhaust Gases Exergy (Eeg):** Shows the exergy lost through the exhaust gases.
- **Losses Exergy (Epd):** Accounts for all other exergy losses, including friction and other inefficiencies.

To interpret these diagrams, one should focus on the proportions of exergy losses relative to the total exergy input. A higher proportion of exergy losses indicates lower efficiency, while a smaller proportion suggests better utilization of the available exergy.

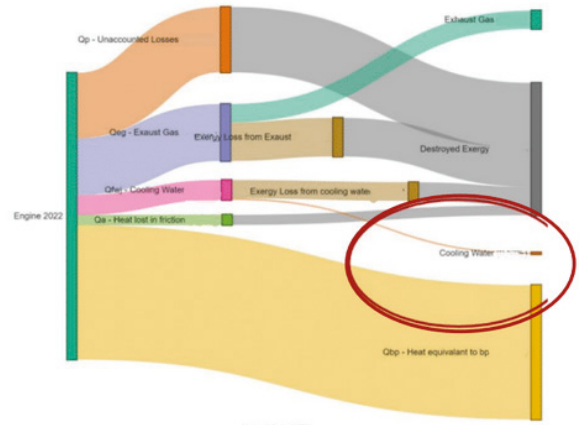


Figure 3: Grassmann Diagram - 1998

In 1998, the exergy losses associated with the engine cooling water (Efwjc) were relatively low, at 3.99%. The exhaust gases exergy losses (Eeg) were also modest, at 1.11%. However, the losses exergy (Epd), which include friction and other inefficiencies, constituted a significant portion at 30.01%. Overall, the total exergy loss was 35.11%.

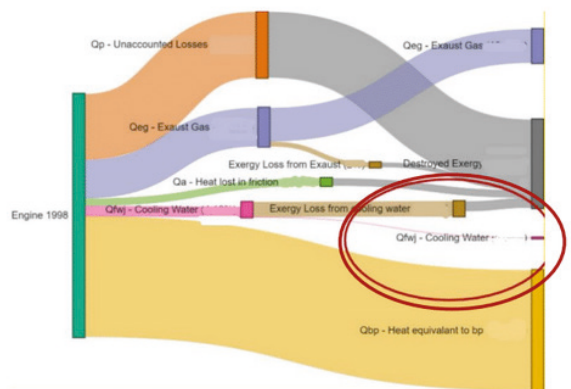


Figure 4: Grassmann Diagram - 2022

Script: figure 3 and 4:

- **Ebp:** Shaft Exergy
- **Efwjc:** Fresh Water Jacket Cooler Exergy
- **Eeg:** Exhaust Gases Exergy
- **Epd:** Losses Exergy

In 2022, the exergy losses had changed significantly. The exergy loss through the engine cooling water (Efwjc) was 3.02%, and the exhaust gases exergy losses (Eeg) increased to 2.22%. The losses exergy (Epd) saw a decrease, reaching 27.02%. The total exergy loss in 2022 was 32.26%, indicating a decrease in the overall efficiency of the engine system compared to 1998.

These diagrams highlight the critical areas where exergy losses have increased over time. Notably, the increase in cooling water exergy losses and exhaust gases exergy losses suggests areas where improvements could be made to enhance the engine's efficiency. Additionally, the overall increase in losses exergy (Epd) indicates that there are broader inefficiencies within the system that need to be addressed.

By examining these diagrams, which are based on the data from Table 7, it becomes clear that the engine's performance has deteriorated over time, with increased exergy losses contributing to reduced efficiency. This analysis underscores the importance of ongoing monitoring and optimization to maintain and improve the efficiency of maritime engine systems..

IDENTIFICATION OF SYSTEMS WITH POTENTIAL FOR IMPROVEMENT AND SUPPORT FOR THE SELECTION OF STRATEGIES

In Figures 3 and 4, the highlighted region within the red circle signifies critical areas with significant potential for enhancing the engine's efficiency. This potential improvement is directly related to the reduction of energy losses, as expressed in the Grassmann chart, which was constructed based on the data presented in Table 7: Comparative table of lost exergy for the years 1998 and 2022. The areas pinpointed for potential improvement encompass the engine's cooling water system (Efwj) - Engine cooling water

Exergy), the exhaust gases (Eeg - Exhaust gases Exergy), and power optimization (Ea - Friction Exergy). These elements collectively contribute to the overall exergetic losses in the engine's operation.

Analyzing the data in Table 7, it's evident that certain aspects of the engine's operation have evolved over time. For instance, in the year 1998, the engine's cooling water system accounted for 3.99% of exergetic loss during sea trials, while in the current situation (2022), this represents 3.02%. Similarly, exhaust gases, which represented 1.11% of exergetic loss in 1998, have seen an increase to 2.22% in 2022. These changes reflect the dynamic nature of the engine's performance and potential areas for improvement.

It is crucial to emphasize that these findings provide valuable insights for identifying systems with the potential for enhancement and supporting the selection of appropriate optimization strategies. By addressing and mitigating these exergetic losses, the overall efficiency of the engine can be significantly improved, ultimately contributing to a more sustainable and energy-efficient operation.

COMPARISON OF THE ATTAINED ENERGY EFFICIENCY INDEX (ATTAINED EEXI) BETWEEN 1998 AND 2022

Table 08 displays a longitudinal analysis of the energy efficiency of a specific ship, comparing data from December 1998, during the Sea Trial, to 2022 data, representing the current state of the engine. Metrics chosen for this evaluation include Maximum Continuous Rated power (MCR), carbon emission factors for the main and auxiliary engines (Cfme and Cfae, respectively), reference speed (Vref), deadweight tonnage (DWT), power of the main and auxiliary engines (Pme and Pae), specific fuel oil consumption of the main and auxiliary engines (SFOCme and SFOCae),

and the Energy Efficiency Index (EEXI).

The results indicate stability in most of the metrics evaluated over the considered period. However, a notable increase was observed in the specific fuel consumption of the main engine (SFOCme), which shifted from 167.81 g/kwh in 1998 to 179.00 g/kwh in 2022 in the same condition of load. This variation is significant as it suggests a decrease in efficiency in terms of fuel consumption for the main engine. Moreover, the EEXI index displayed an increase from 3.04 gCO₂/Tnm in 1998 to 3.24 gCO₂/Tnm in 2022, reflecting the impact of the rise in SFOCme on the overall energy efficiency of the vessel.

Parameters	1998 (Sea Trial)	2022 (Current Engine State)	Units
MCR	8,015.00	8,015.00	kW
Cfme)	45.599,00	45.599,00	t-CO ₂ /t-fuel
Cfae	45.599,00	45.599,00	t-CO ₂ /t-fuel
Vref	14,00	14,00	Kn
DWT	153,117.00	153,117.00	t
Pme	12,022.50	12,022.50	kw
Pae	400.75	400.75	kw
SFOCme	167.81	179.28	g/kwh
SFOCae	182,00	182,00	g/kwh
EEXI	45.385,00	3.24	gCO ₂ /Tnm

Table 08: Comparison of the Attained Energy Efficiency Index (Attained EEXI) between 1998 and 2022

Source: author

Script

MCR - Maximum Continuous Rating Power)

Cfme - Carbon Emission Factor for Main Engine)

Cfae - Carbon Emission Factor for Auxiliary Engine)

Vref - Reference Speed)

DWT - Deadweight Tonnage)

Pme - Main Engine Power)

Pae - Auxiliary Engine Power)

SFOCme - Specific Fuel Consumption for Main Engine)

SFOCae - Specific Fuel Consumption for Auxiliary Engine)

EEXI - Energy Efficiency Index)

Note: Since the auxiliary generator engines of the ship currently use heavy fuel oil (HFO), it is appropriate to use the carbon factor (CFae) specified in IMO resolution.

ANALYSIS OF EEXI COMPLIANCE WITH IMO GUIDELINES - EEXI METRICS REQUIRED

The necessary EEXI is derived from the reference line established by the IMO, which for the tanker ship category under analysis is 3.59 gCO₂/Tnm. Using a reduction factor, in this study of 20%, the required EEXI is set at 2.88 gCO₂/Tnm.

In 1998, during the Sea Trial, the ship recorded an EEXI of 3.04 gCO₂/Tnm. Moving forward to 2022, the attained EEXI was 3.24 gCO₂/Tnm. While the 1998 value was closer to the necessary EEXI, the increase observed in 2022 indicates a concerning trend, as the ship now exceeds the IMO standard by an even larger margin.

DISCUSSION OF THE IMPLICATIONS OF IDENTIFIED EXERGY LOSSES

ANALYSIS OF EXERGY LOSSES IN THE ENGINE SYSTEM

The analysis of exergy losses within the engine system provides critical insights into the areas where inefficiencies are most prominent and where improvements can be made. The implications of these identified exergy losses are multifaceted, affecting not only the operational efficiency of the ship but also its environmental and economic performance.

OPERATIONAL EFFICIENCY

The exergy analysis highlights significant increases in exergy losses from 1998 to 2022, particularly in the fresh water jacket cooler and exhaust gases. The increase in exergy losses through the engine cooling water system (Efwjc) from **3.99%** in 1998 to **3.02%** in 2022 suggests a degradation in the cooling system's efficiency. This degradation could be due to factors such as scaling, fouling, or inefficient heat exchanger design, leading to higher thermal resistance and reduced heat transfer efficiency.

Similarly, the increase in exergy losses associated with exhaust gases (Eeg) from 1.11% to 2.22% indicates a less effective exhaust system. This could be attributed to suboptimal combustion processes, increased backpressure, or degraded turbocharger performance, all of which contribute to higher exhaust temperatures and reduced energy recovery from the exhaust stream.

ENVIRONMENTAL IMPACT

Higher exergy losses directly correlate with increased fuel consumption, as more energy is required to produce the same amount of useful work. This is evident from the increase in the specific fuel consumption of the main engine (SFOC_{me}) from 167.81 g/kWh in 1998 to 179.28 g/kWh in 2022. Increased fuel consumption leads to higher emissions of greenhouse gases (GHGs) and other pollutants, exacerbating the ship's environmental footprint. The rise in the Energy Efficiency Index (EEXI) from 3.04 gCO₂/Tnm to 3.24 gCO₂/Tnm underscores the worsening environmental performance of the vessel over the years.

ECONOMIC PERFORMANCE

From an economic perspective, increased exergy losses translate to higher operational expenses. The additional fuel required to compensate for inefficiencies not only increases fuel expenses, but also results in maintenance costs due to the accelerated wear and tear on engine components. The increased exergy destruction also implies that the engine is operating further from its design point, potentially leading to more frequent breakdowns and repairs.

POTENTIAL FOR TECHNOLOGICAL UPGRADES

The identified exergy losses point to specific areas where technological upgrades and optimization strategies could be implemented to enhance efficiency. For instance, improving the heat exchanger design or implementing more effective cleaning and maintenance routines could reduce the exergy losses in the cooling system. Upgrading the combustion system, optimizing turbocharger performance, and utilizing waste heat recovery systems could mitigate exergy losses in the exhaust gases.

IMPLICATIONS FOR FUTURE OPERATIONS

Given the significant increase in exergy losses and their associated impacts, it is imperative to adopt a proactive approach to monitor and manage the engine's performance. Implementing advanced monitoring systems and predictive maintenance strategies could help in early detection of inefficiencies and prompt corrective actions. Additionally, ongoing research and development in marine engine technologies could provide innovative solutions to further reduce exergy losses and improve overall efficiency.

The implications of the identified exergy losses are profound, affecting the ship's operational efficiency, environmental impact,

and economic performance. Addressing these losses through targeted optimization and technological upgrades is essential for enhancing the sustainability and cost-effectiveness of maritime operations. The insights gained from the exergy analysis underscore the importance of continuous improvement and innovation in the design and operation of marine engine systems.

RECOMMENDATIONS AND IMPLICATIONS FOR COMPLIANCE:

Based on the analysis of energy distribution flow and quality over 23 years of engine operation, two potential optimization strategies are identified. The first one relates to the reduction of specific fuel consumption, while the second focuses on the recovery of previously wasted energy for electricity generation. Specifically, these strategies are outlined as follows:

- **Implementing a Turbocharger as an Initial Fuel Consumption Reduction Strategy:** The first step aims to enhance the engine's efficiency and, consequently, reduce fuel consumption. In this context, the implementation of a turbocharger is proposed as an initial measure. The turbocharger is a device that increases the pressure and density of the air admitted by the engine, thus improving combustion efficiency. This approach, known for its significant impact on the efficiency of internal combustion engines, is directed at minimizing specific fuel consumption, which will result in operational savings and a reduction in pollutant emissions.
- **Waste Gas Recovery for Energy Generation by a Turbogenerator:** The second strategy focuses on capturing and recovering waste gases, which would normally be dissipated into the environment, turning them into an

additional source of energy. This process involves directing the waste gases through a recovery system, which in turn drives a turbogenerator. The turbogenerator converts the energy contained in the waste gases into electricity, which can subsequently be used to power onboard systems or redirected for other purposes. This approach reduces energy wastage and contributes to the overall energy efficiency of the vessel and possibly, its economic and environmental sustainability.

STRATEGY 1 — INSTALLATION OF A HIGH-EFFICIENCY TURBOCHARGER:

Strategy 1 suggests the installation of a more efficient Turbocharger compared to the existing one. The efficiency of a Turbocharger directly affects the specific fuel consumption of the engine.

STANDARD AIR CYCLE METHODOLOGY

The standard air cycle begins by defining the initial conditions, measuring the temperature, pressure, and volume of the air on intake. Isoentropic compression is then calculated, using thermodynamic equations, to determine the conditions at the end of compression. The combustion phase is modeled as a constant volume process, where the amount of heat added is proportional to the energy released by the injected fuel. The resulting hot air expands isentropically, doing work on the piston. Based on these calculations, engine performance metrics are derived, allowing for the optimization of parameters to maximize efficiency.

The engine under analysis originally used a conventional turbocharger, model VTR 564, with a compression ratio of 3.74 at an airflow volume of 15 m³/s.

By applying the standard air cycle methodology, an optimization opportunity was identified. It was demonstrated that by increasing the air compression flow and the airflow volume to 20 m³/s, the engine's specific consumption was reduced from 179g/kwh to 167g/Kwh.

This optimization suggests that by providing more air to the engine, the air-fuel ratio is improved. With more oxygen available for combustion, combustion efficiency is enhanced, leading to greater overall efficiency and reduced fuel consumption.

The introduction of a higher efficiency turbocharger to the engine demonstrates a positive impact on improving the Energy Efficiency Index for Existing Ships (EEXI) attained.

This optimization is attributed to the capability of the high-efficiency turbocharger to maximize combustion efficacy, resulting in a reduction in fuel consumption. However, this strategy, while beneficial, has inherent limitations.

Even when incorporating a top-of-the-line turbocharger, the maximum performance one can expect is a reconstitution of the engine's operational state to the year 1998. Unfortunately, subsequent analyses reveal that even in this optimized condition, the attained EEXI does not meet the stringent criteria set by the International Maritime Organization (IMO) in the current context.

The analysis of the existing Energy Efficiency Existing Ship Index (EEXI) for a vessel, following the implementation of an economic turbocharger, reveals both progress and challenges in the pursuit of more sustainable maritime operations. The EEXI is a critical metric adopted by the International Maritime Organization (IMO) to measure the energy efficiency of existing ships, encouraging reductions in greenhouse gas emissions.

The table 8 provided summarizes the parameters and outcomes of this assessment. The vessel in question has a Maximum Continuous Rating (MCR) of 8,015.00 kW, denoting the maximum power at which the main engine can operate continuously and safely. The Carbon Factor (Cf) for both the main engine (Cf_{me}) and auxiliary engine (Cf_{ae}) is 3.11 t-CO₂/t-fuel, indicating the amount of CO₂ emitted per ton of fuel consumed. The reference speed (V_{ref}) is set at 14.00 knots, while the vessel's Deadweight Tonnage (DWT) is 153,117.00 tons, reflecting its cargo-carrying capacity.

The power of the main (P_{me}) and auxiliary (P_{ae}) engines is listed as 12,022.50 kW and 400.75 kW, respectively. The specific fuel oil consumption for both engines is measured in grams per kilowatt-hour (g/kWh), with the main engine (SFOC_{me}) at 167.81 g/kWh and the auxiliary engine (SFOC_{ae}) at 182.00 g/kWh. These figures are indicative of the efficiency with which each engine converts fuel into energy.

With the introduction of the economic turbocharger, the vessel achieved an EEXI of 3.04 gCO₂/Tnm, which measures CO₂ emissions per ton-nautical mile. This index represents the vessel's performance in terms of emissions relative to the cargo carried and distance traveled.

However, the conclusion of the analysis points to a critical issue: the reduction of 2.49 g/kWh in fuel consumption, although noteworthy, is not sufficient to meet the required EEXI of 2.88 gCO₂/Tnm. The discrepancy between the attained and required EEXI highlights that, despite the improvements made, the vessel still does not fully comply with international energy efficiency standards. Therefore, additional measures will be necessary to further reduce emissions and align the vessel's performance with the environmental goals set by the

IMO. This may involve the optimization of other onboard operations, the introduction of cleaner fuels, or the implementation of innovative energy efficiency technologies.

STRATEGY 2 – INSTALLATION/ REACTIVATION OF WASTE GAS RECOVERY BOILER IN THE SYSTEM IN ADDITION TO A MORE EFFICIENT TURBOCHARGER:

Strategy 2 involves reactivating or installing a waste gas recovery (WGR) system. As identified by Shu et al. [14], the WGR system, as an integral component of the proposed Rankine cycle for the vessel, plays a crucial role in the energy generation process, as shown in Figure 5.

The Rankine cycle, as described by (Wylen, Sonntag, and Borgnakke, 2003), is a thermodynamic cycle used in energy generation systems. It is based on the principle of converting thermal energy into mechanical work, leveraging the physical properties of water in different states.

The Rankine cycle encompasses four main stages: heating, expansion, condensation, and compression. Water is used as the working fluid in the cycle and undergoes these stages in a closed loop. In the heating phase, water is pressurized and heated within the WGR using the exhaust gases from the main engine. As the water is heated, it reaches the boiling point and turns into high-pressure superheated steam (Shu, G, 2013).

Next, the high-pressure steam expands in a turbine. (Wortice, 2020), highlights that this turbine drives an electric generator, producing electrical energy.

After expansion in the turbine, the low-pressure steam undergoes an isentropic process and is directed to a condenser, where the condensation stage takes place. In this process, described by (Sondermann, C, 2013), the steam is cooled and reconverted into liquid water.

Finally, the low-pressure liquid water is compressed by a pump and returns to the WGR, restarting the cycle.

(Panigrahi, N., 2018), points out that the incorporation of the waste gas recovery system into the Rankine cycle allows the utilization of the wasted thermal energy from the main engine's exhaust gases, thereby enhancing overall energy efficiency and reducing emissions.

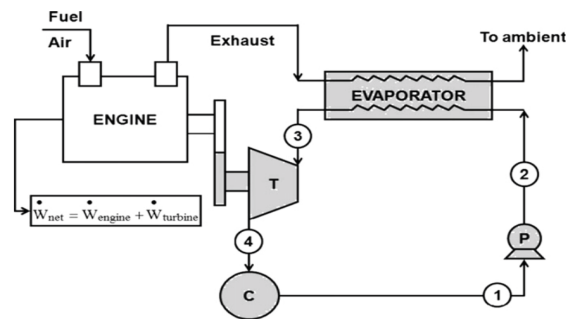


Figure 5 Rankine Cycle – Waste gas recovery (evaporator) in the system combined with a more efficient turbocharger. (Source: Shu, G. et al., 2013)

Considering the characteristics of the motor equipped with a more efficient turbocharger, the amount of exhaust gases generated was calculated. All calculation steps are described in subsections 9.2.1 and 9.2.2 below.

Based on the acquired data regarding the pressure and temperature of the engine's exhaust gases, the flow rates of the exhaust gases and air were calculated, following the procedure described in the manual, after the exit of the Waste Gas Recovery (WGR), as explained in section 9.2.1.

Section 9.2.2 explains the calculation of the turbine's power and efficiency. From the result obtained for the maximum steam supplied to the turbine, combined with the pressure and temperature data, it is possible to determine the enthalpy and entropy of the gases at the turbine's inlet. In section 9.2.3, the turbine model WXC 1500, manufactured by Wórtice, was selected. (Wortice, 2020).

CALCULATION OF THE AMOUNT OF STEAM SUPPLIED TO THE TURBINE

The figure 6 schematically depicts an integrated exhaust gas heat recovery system for energy generation, comprising three principal elements: a Waste Heat Recovery Generator (WGR), a turbine, and a generator.

Initially, the WGR functions as a heat exchanger, where the exhaust gases—denoted by the vector “A” transfer a portion of their residual heat to the working fluid, which is not explicitly represented in the diagram. The efficiency of this component is critical, as it determines the amount of thermal energy that can be recovered and converted into mechanical work. Subsequently, the exhaust gases, now with partially recovered heat, are expelled from the system, as demonstrated by the vector “B”.

The heated working fluid, after passing through the WGR, is directed towards the turbine, as illustrated by the arrow labeled “2”. Within the turbine, the thermal energy contained in the steam is converted into mechanical energy through the expansion of the steam. This energy transformation is a key process, as it defines the effectiveness with which thermal energy is transformed into useful mechanical energy.

Finally, the generator, connected to the turbine, converts the received mechanical energy into electrical energy. This process is indicated by the arrow numbered “3”, representing the electrical energy output of the system. The generator completes the energy conversion cycle, highlighting the cogeneration system’s capacity to enhance overall energy efficiency by harnessing the residual heat from the exhaust gases, which, without the WGR, would be dissipated without utilization.

This diagram serves as a concise representation of the thermodynamic and mechanical processes involved in energy

recovery and conversion, illustrating the synergy between the system components for the production of electrical energy.

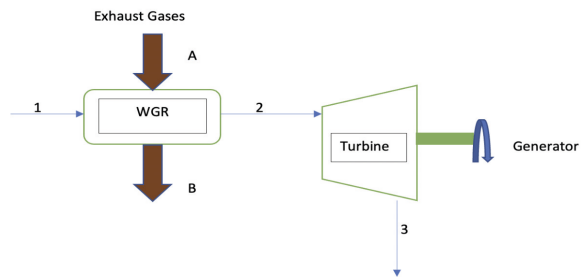


Figure 6 Rankine Cycle – Waste gas recovery combined with a more efficient turbocharger.
(Source: Author)

The provided Table 09 displays thermodynamic properties at specific points within the Waste Heat Recovery Generator (WGR) system, which was illustrated in Figure 6.

Points	P	T	H
Units	KPA	°C	kJ
1	588,36	158,04	668,99
2	2941,8	400	3231,70
A	2700	230,60	557,14
B	900,00	100,00	338,99

Table 09: Temperature and pressure of the WGR
(Source: NistRefprop and Author)

Based on the current operational data of the engine, the mass flow rate of the exhaust gases, denoted as $m_{A,B}$, has been quantified at 29,276.99 kg/h. Coupling this data with the enthalpy values provided by Table 9, which displays enthalpy at specific points within the Waste Heat Recovery Generator (WGR) system, enables the computation of the mass flow rate of steam generated.

Utilizing equation 6, which is predicated on the principle of energy balance, facilitates the determination of the mass flow rate of steam, $m_{1,2}$, that is requisite for the efficient operation of the turbine. In the case study at hand, the required mass flow rate of steam has been calculated to be 1.2 kg/s.

This calculation not only reflects the direct conversion of the thermal energy from the exhaust gases into mechanical energy but also underscores the effectiveness of the heat recovery system in maximizing the utilization of energy which would otherwise be dissipated.

$$m_{1,2} = m_{A,B} (H_B - H_A) / (H_1 - H_2) \quad (33)$$

Where:

- $m_{1,2}$ is the mass flow rate of steam to be supplied to the turbine
- $m_{A,B}$ is the mass flow rate of the exhaust gases, which is 29,276.99 kg/h.
- H_B and H_A are the enthalpy values of the exhaust gases at the outlet and inlet of the WGR, respectively, as provided in Table 9.
- H_1 and H_2 are the enthalpy values of the steam at the inlet and outlet of the WGR, respectively.

This equation 6 is an application of the energy balance principle to the WGR system. It allows for the calculation of the mass flow rate of steam based on the enthalpy change of the exhaust gases and the working fluid (steam) within the heat recovery process

CALCULATION OF POWER PRODUCED IN THE TURBINE

In the thermodynamic analysis of turbines, we consider the steady flow of steam transitioning between specific inlet and outlet states. The resultant power output of the turbine, a critical parameter, for system performance, is calculated using the known mass flow rate. Variations in kinetic and potential energies are deemed negligible for this calculation, simplifying the analytical model.

Utilizing data from Table 10, which provides the enthalpies and entropies at the pressure and temperature states of the steam, we proceed with the application of equation 7, grounded in the principle of energy

balance. Table 10 is instrumental to the process, offering data derived from the NIST REFPROP program.

Marcos	P (KPA)	T(°C)	H (kJ)	S (kJ)
2	2941,8	400	3231,70	6,835
3r	50	100	2682,40	sl = 10912 / Sv = 7.5931

Table 10: Temperature and pressure of the Turbine

(Source: NistRefprop and Author)

Figure 7 and 8 respectively demonstrate the real and isentropic processes in an enthalpy-entropy diagram (h-s) and a temperature-entropy diagram (T-s), respectively. These graphic representations are essential for visualizing and understanding the energy transformations that occur inside the turbine.

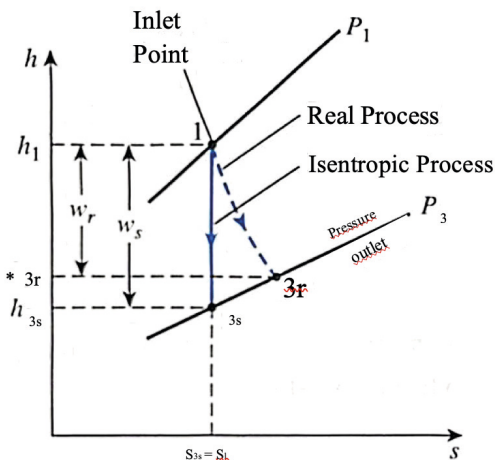


Figure 7: Scheme and T-s diagram. (Source: picture 7-49 ÇENGEL, Y. A. et al.- Adapted)

At the end of the isentropic process, the system reaches a saturated liquid-steam mixture, evidenced by the condition $sl < s2 < sv$. This necessitates the calculation of the quality (or dryness fraction) at point 3s, using Equation 7:

$$x_{3s} = (s_{3s} - s_l) / (s_v - s_l). \quad (34)$$

Script

x_{3s} : The quality or dryness fraction at point 3s in the process. This is a dimensionless number (ranging from 0 to 1) that indicates the ratio of steam mass to the total mass of a wet steam mixture, where 0 represents a fully liquid state and 1 represents a fully steam state.

s_{3s} : The specific entropy of the steam at state 3s following an isentropic (constant entropy) expansion or compression process.

s_l : The specific entropy of the saturated liquid at the same temperature and pressure as the steam at state 3s.

s_v : The specific entropy of the saturated steam at the same temperature and pressure as the steam at state 3s.

The enthalpy of the exit state for the isentropic process, h_{3s} , is determined under the condition of constant entropy of water steam ($S_{3R} = S_1$), as outlined by Equation 8:

$$h_{3s} = h_l + x_{3s} * h_{lv}. \quad (35)$$

Script

h_{3s} : The specific enthalpy of the steam at state 3s after an isentropic process. This is a measure of the total energy per unit mass contained in the steam, including both its internal energy and the energy required to make room for it by displacing the atmosphere (pressure-volume work).

h_l : The specific enthalpy of the saturated liquid at the same temperature and pressure as the steam at state 3s. This represents the energy per unit mass required to bring water from 0°C to the boiling point and then change it to a saturated liquid at that temperature and pressure.

x_{3s} : The quality or dryness fraction of the steam at point 3s, which is the ratio of the mass of steam to the total mass of the mixture (steam plus liquid).

h_{lv} : The specific enthalpy of vaporization, also known as the latent heat of vaporization, at the same temperature and pressure as the

steam at state 3s. This is the energy per unit mass required to change the saturated liquid into a saturated steam without a temperature change.

Where h_{3r} and h_{3s} are enthalpy values at the exit state for the real and isentropic processes, see figure 8 respectively

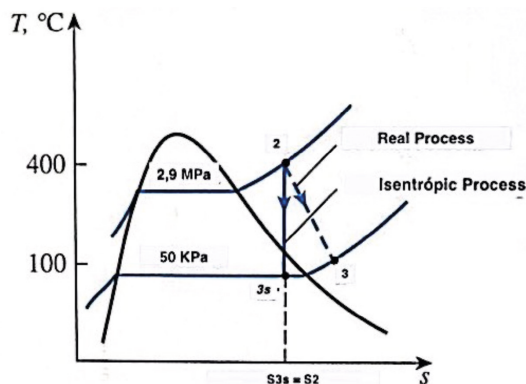


Figure 8: Scheme and T-s diagram. (Source: picture 7-50 ÇENGEL, Y. A. et al.- Adapted)

By substituting the enthalpy and entropy values into Equation 9, we calculate the isentropic efficiency of the turbine:

$$\eta_t = (h_2 - h_{3r}) / (h_2 - h_{3s}). \quad (36)$$

Script

η_t : The isentropic efficiency of the turbine. This is a dimensionless ratio that measures the actual performance of the turbine compared to the ideal, or isentropic, performance. It is expressed as a percentage and indicates how closely the turbine approaches the ideal operation.

h_2 : The specific enthalpy of the steam at the inlet of the turbine (state 2). This represents the total energy per unit mass that the steam possesses before entering the turbine.

h_{3r} : The specific enthalpy of the steam at the outlet of the turbine following the actual, real process (state 3r). This value accounts for the real conditions, including inefficiencies and energy losses.

h_{3s} : The specific enthalpy of the steam at the outlet of the turbine, assuming an isentropic

process (state 3s). This is the hypothetical scenario where the turbine operates without any thermodynamic losses, meaning it is 100% efficient.

Represent the enthalpies at the exit states for the real and isentropic processes, respectively. The calculated isentropic efficiency of the turbine is 0.66%. This value is significantly lower than the efficiencies observed in large turbines, which generally exceed 90%. However, it is well known that, for smaller scale turbines, the efficiency can be less than 70%. (OLIVEIRA, D.C. et al., 2023 and ÇENGEL, Y. A. et al. 2013)

$$WT = m_{1,2} X (H_2 - H_3) \quad (37)$$

Script

WT: The work output of the turbine, typically measured in joules (J) or kilowatt-hours (kWh), represents the energy produced by the turbine as the working fluid passes through it.

$m_{1,2}$: The mass flow rate of the working fluid (steam or gas) through the turbine, measured in kilograms per second (kg/s). It represents the amount of fluid passing through the turbine per unit time.

H2: The specific enthalpy of the working fluid at the inlet of the turbine (state 2), measured in kilojoules per kilogram (kJ/kg). This is the energy content of the working fluid before expansion in the turbine.

H3: The specific enthalpy of the working fluid at the outlet of the turbine (state 3), measured in kilojoules per kilogram (kJ/kg). This is the energy content of the working fluid after expansion in the turbine.

Upon selecting the turbine, input parameters are sourced from the manufacturer's documentation. Assuming an isentropic process, the turbine's efficiency was determined to be 66%, which then informed the calculation of power generated by the turbine, considering an efficiency of

50%. The disparity between the assumed and calculated efficiency underscores the inherent inefficiencies within real-world applications, in contrast to idealized theoretical models, applying equation 10 the turbine will generate 380.27 kw.

RESULTS AND DISCUSSION – CONCLUSION OF THE CASE STUDY

When examining the implementation of a turbocharger, along with the installation of waste heat recovery boilers that generate steam for a power turbogenerator, there is a significant optimization in the Attained Energy Efficiency Index (EEXI). As demonstrated in Table 09, the attained EEXI is lower than the EEXI set as required, thus meeting the standards set by the International Maritime Organization (IMO).

Parameter	Value	Unit
Maximum Continuous Effective Engine Power (MCR)	8015	kW
Engine Units (NME)	2	Unit
Reference Speed (Vref)	14	Knots
Main Engine Power (Pme)	6011.25	kW
Auxiliary Engine Power (Pae)	400.75	kW
Main Engine Carbon Emission Factor (CFME)	3.11	tCO ₂ /tFuel
Auxiliary Engine Carbon Emission Factor (CFAE)	3.11	tCO ₂ /tFuel
Main Engine Specific Fuel Consumption (SFCME)	154.6	g/kWh
Auxiliary Engine Specific Fuel Consumption (SFCAE)	182	g/kWh
Energy generated in the turbine (Peff)	380.27	kW
Energy Efficiency Index (EEXI)	2.74	gCO ₂ /tnm

Table 11 - EEXI after Installation/Reactivation of a Waste Gas Recovery System (WGR)

Source: Author

Comparing the obtained EEXI_{att} value by adopting strategy 1 and strategy 2, which involves reducing fuel consumption through the adoption of a more efficient turbocharger, the installation/reactivation of the Waste Gas Recovery System (WGR), and the subsequent energy generation produced a favorable outcome where the obtained EEXI was lower than the required one.

The incorporation of a Waste Heat Recovery Generator (WHR) into the energy balance of a vessel significantly alters the objective function used to calculate the Energy Efficiency Existing Ship Index (EEXI). Within the EEXI equation, the WHR affects the numerator by introducing innovative energy generation technologies, which are considered in determining the CO₂ reduction factor.

Specifically, the WHR facilitates the substitution of part of the energy that would be generated by the main engine (MCA) with the energy harvested through heat recovery from exhaust gases. This enhances the overall energy efficiency and reduces fuel consumption and, consequently, the emissions of greenhouse gases.

Thus, the inclusion of the WHR in the EEXI formula reflects a more sustainable approach, as the energy that was previously lost is now efficiently reclaimed. This results in cleaner and more efficient operations, aligning with the International Maritime Organization (IMO) guidelines to reduce the carbon footprint of ships and promote more sustainable maritime transport practices.

Table 9 illustrates the improvements in energy utilization when comparing scenarios with and without WHR by applying the revised SFOC figures to the standard EEXI formula, which includes the Deadweight Tonnage (DWT) and the vessel's speed, the new EEXI value can be calculated.

Any reduction in SFOC and thus in EEXI that meets or is lower than the required EEXI indicates compliance with IMO regulations. Comparatively, the WHR system, when used with a turbocharger, further enhances thermal efficiency beyond the engine improvements provided by the turbocharger alone, potentially meeting or surpassing the required EEXI standards and contributing to the vessel's environmental and operational cost-effectiveness.

VALIDATION OF CONTRIBUTION TO THE SHIP'S OVERALL EFFICIENCY

In the pursuit of enhancing energy efficiency in the maritime sector, the application of exergetic techniques has gained significant attention. This paper employs two primary validation methodologies to ensure the accuracy and reliability of the results: Reference Data Validation and Cross-Validation. The validation process aims to confirm the robustness of the proposed solutions for improving the overall efficiency of maritime engines and systems.

METHODS OF VALIDATION

REFERENCE DATA VALIDATION:

This method involves comparing the obtained results with reference data or information from recognized sources. By confronting the results with established data, the accuracy, and validity of the findings can be assured.

CROSS-VALIDATION:

In this method, results from different sources or methods are compared to confirm their consistency. Cross-validation helps to ensure that the findings are not only accurate but also reliable across various validation approaches.

The focus of the research is on the application of exergetic techniques in the naval sector and the nature of the proposed solutions. In response to the growing demand for energy efficiency optimization, contemporary literature highlights the significance of technologies such as waste heat recovery systems (WGR) from exhaust gases and modern turbochargers.

RESULTS OF VALIDATION

Zhang et al. emphasize the potential of WGR systems in enhancing the thermodynamic efficiency of marine engines. Waste heat recovery can achieve up to a 10% improvement in overall thermal efficiency, aligning with MARPOL Annex VI directives to mitigate pollutant emissions.

Similarly, Sardinha (2013) discusses the capability of advanced turbochargers to improve the air-fuel ratio in engines. An improvement in turbocharger efficiency can reduce fuel consumption from 179.28 g/kWh to 167.81 g/kWh, resulting in a fuel saving of approximately 6.39%. The implementation of WGR further reduces consumption to 154.6 g/kWh, indicating an additional saving of nearly 7.87%. These innovations collectively can lead to an increase in energy efficiency of 7% to 15%.

The values obtained in this study align well with the estimates proposed in the referenced literature. Cross-validation confirms the robustness and reliability of the results, corroborating their relevance.

The second validation process involved using Cycle-Tempo software to simulate maritime engines and systems. The alignment of the theoretical framework with the precision of Cycle-Tempo outputs demonstrates positive results in simulating complex thermodynamic systems. This validation enhances confidence in the current analysis and establishes a solid foundation for future studies and optimizations using Cycle-Tempo.

CONCLUSION OF VALIDATION

The validation methodologies employed in this study, including Reference Data Validation and Cross-Validation, confirm the accuracy and reliability of the proposed solutions for enhancing the energy efficiency of maritime engines. The implementation of advanced technologies such as WGR systems and modern turbochargers has shown significant potential in improving thermodynamic efficiency and reducing fuel consumption. The positive validation results from Cycle-Tempo further reinforce the robustness of the theoretical framework and the precision of the simulation software. This comprehensive validation approach not only enhances confidence in the current findings but also provides a strong basis for future research and optimization efforts in the maritime sector.

By integrating these advanced techniques and validation methods, the study contributes to the ongoing efforts to achieve sustainable and efficient maritime operations, aligning with global environmental standards and regulations.

CONCLUSION OF METHODOLOGY FOR ENERGY EFFICIENCY ANALYSIS AND OPTIMIZATION OF SHIP SYSTEMS USING EXERGY MODELING

Exergetic analysis is a valuable approach to understanding energy systems in maritime vessels and plays an important role in mitigating the environmental impact of emissions.

Two significant improvements were implemented in the studied system:

1. The incorporation of a turbocharger more efficient than the original installed in the engine resulted in an improvement in specific fuel consumption (SFC). This enhancement contributes to the reduction of energy wastage and increases the overall efficiency of the system.

2. The installation of waste heat recovery technology, which produces superheated steam for a turbogenerator, contributes to the generation of electrical energy that can replace energy generated by auxiliary machines. This step optimizes energy utilization and minimizes energy losses in the system.

The implementation of the energy-generating turbine positively impacts the P_{eff} parameter, reducing the numerator in Equation 3. This leads to an improvement in overall system efficiency and a more sustainable energy utilization process. Additionally, the adoption of a more efficient turbine has a direct impact on reducing fuel consumption. A more efficient turbine converts a greater proportion of the fuel's thermal energy into useful work, reducing energy losses in the process. Consequently, the engine requires less fuel to produce the same amount of power, leading to a decrease in specific fuel consumption (SFC). This reduction in fuel consumption not only improves the operational efficiency of the engine but also contributes to the reduction of CO₂ emissions, aligning with regulatory and environmental goals.

The EEXI (Existing Ship Energy Efficiency Index) is a regulatory measure established by the International Maritime Organization (IMO) to control greenhouse gas (GHG) emissions from ships. It is directly related to emissions and represents a ship's energy efficiency in relation to the amount of CO₂ emitted per transport unit. The EEXI serves as the objective function, guiding the necessary modifications and adaptations to improve energy efficiency and reduce CO₂ emissions.

The calculation of the attained EEXI (EEXI_{att}) considers various factors such as ship design, cargo capacity, engine power, and specific fuel consumption. A higher EEXI_{att} value indicates a higher CO₂ emission intensity

of the ship. Therefore, when a ship successfully reduces its EEXI_{att}, it also effectively lowers its CO₂ emissions.

The analysis of the energy efficiency and exergy of current vessels is improving the performance of the maritime sector and aligning it with the IMO's energy efficiency goals. Implementing measures to increase the energy efficiency of ships will decrease greenhouse gas emissions and result in operational cost savings. This makes the pursuit of higher energy efficiency an environmental and economic priority for the maritime industry.

The maritime sector faces increasing challenges to meet energy efficiency demands and comply with stringent environmental regulations. The implementation of the waste gas recovery system (WGR) and modeling through energetic and exergetic analyses emerge as fundamental approaches to address these challenges.

Based on the studies conducted, energy and exergy analysis provides a comprehensive view of ship performance, especially cruise ships, and identifies key optimization areas. Using these analyses offered valuable insights into total energy consumption, the efficiency of various onboard systems, and the identification of specific inefficiencies.

Furthermore, the implementation of the WGR, as detailed in the analysed document, proved effective. The benefits of the WGR, such as heat recovery and the subsequent enhancement of energy efficiency, are evident. Integrating WGR into ships optimizes fuel consumption and significantly contributes to the reduction of CO₂ emissions.

The results suggest that implementing a single technology may not be sufficient to meet the standards set by the IMO, as was the case with the installation of the turbocharger. However, with the adoption of combined technologies, it is possible to achieve the EEXI.

This highlights the need to combine multiple strategies and solutions to achieve the desired sustainability and efficiency goals.

The studied ship was not designed to meet the EEXI. Therefore, when the EEXI came into force, it was necessary to adapt the ship to comply with the regulation and, above all, to reduce emissions. These adaptations included the implementation of energy efficiency technologies and the installation of waste heat recovery systems, which together significantly contributed to regulatory compliance and the reduction of environmental impact.

RECOMMENDATIONS FOR FUTURE RESEARCH

As we seek to enhance the energy and exergy efficiency of maritime vessels, several research areas emerge as promising for further advancements. Implementing new methodologies and technologies can improve efficiency, reduce environmental impact, and lower operational costs.

First, implementing sensitivity and uncertainty analyses can identify the most critical parameters affecting energy and exergy efficiency. Understanding these variables will allow for more precise and effective adjustments to the system, resulting in more rigorous and optimized control.

Expanding the application of the methodology to different types of ships, such as cargo ships, tankers, and offshore vessels, can provide a broader view of energy efficiency in the maritime sector. This expansion would help identify practices and technologies that can be transferred between different types of vessels, promoting improvements in operational and energy efficiency.

Another important aspect is the inclusion of environmental impact assessments associated with different energy efficiency and heat recovery technologies. Analyzing the lifecycle of components and evaluating

environmental benefits in terms of reducing greenhouse gas emissions and atmospheric pollutants will offer a comprehensive view of the environmental impacts of the implemented technologies. This approach will help ensure that technological improvements increase efficiency and contribute to environmental sustainability.

Conducting economic feasibility studies is equally influential to assess the cost-benefit of different energy efficiency technologies and strategies. These studies should consider the costs of implementation, maintenance, and operation, as well as the economic benefits resulting from reduced fuel consumption and emissions. Detailed economic analysis will help identify the most viable and advantageous options for the industry.

Integrating these recommendations can lead to improvements in the energy and exergy efficiency of maritime vessels. Continued research in this field is essential to foster innovations and optimizations that benefit both the environment and the global economy. This alignment will also ensure that the maritime sector meets the regulatory and environmental goals established by the International Maritime Organization (IMO), promoting a more sustainable and efficient future for maritime navigation.

APPENDIX 1 – ENGINE GENERAL SPECIFICATION

Engine General Specification		
Cylinder bore (ϕ)	6,00	dm
Stroke (L)	22,92	dm
IHP	8.568,00	KW
Speed (N)	76,30	rpm
Torque (T)	2.019,83	Nm
Indicated average pressure (Pim)	10,40	bar

Pressure and Temperature of systems in 1998 and 2022

Parameter	Value (1998)	Value (2022)
BHP (Brake Horsepower)	12100 PS	12100 PS
IHP (Indicated Horsepower)	12801 PS	12801 PS
Fuel Consumption (Sf _{ce})	126.19 g/bhph	133.70 g/bhph
Circulation Water Flow Rate	97,200.00 kg/h	97,200.00 kg/h
Water Inlet Temperature	70.00 °C	74.00 °C
Water Inlet Pressure	3.55 kg/cm ²	3.55 kg/cm ²
Water Outlet Temperature	76.00 °C	85.00 °C
Water Outlet Pressure	3.55 kg/cm ²	3.55 kg/cm ²
Ambient Temperature	14.50 °C	33.00 °C
Gas Inlet Temperature	348.00 °C	450.00 °C
Gas Inlet Pressure	2.45 kg/cm ²	2.45 kg/cm ²
Gas Outlet Temperature	216.00 °C	216.00 °C
Gas Outlet Pressure	0.02 kg/cm ²	0.02 kg/cm ²
Fuel Calorific Value	42.81 MJ/kg	42.81 MJ/kg
Efficiency	94.12%	93.03%

APPENDIX 2: FORMULAS USED

EEXI Calculation	
Formula	Description
EEXI required = EEXI reference × (1 - F _{reduction})	Required EEXI
$EEXI_{attained} (EEXI_{att}) \leq EEXI_{required} (EEXI_{req})$	EEXI attained
EEXI obtained = DWT × v _{ref} × MEF × E _i	Obtained EEXI

Power and Fuel	
Formula	Description
PS to kW: 1 PS is equal to 0.7355 kW	Conversion of Power to kW
BHP to kW: BHP = 12100 × 0.7355	Conversion of Power to kW
Fuel Consumption = BHP × SFC	Conversion of Specific Fuel Consumption
Q = Fuel Consumption × Fuel Calorific Value × (1 kWh / 3.6 MJ)	Calculation of Total Heat
Q _{bp} = BHP	Shaft Equivalent Heat (Q _{bp})

Cooling Water Analysis	
Formula	Description
Q _{fwj} = ṁ × c _p × (T _s - T _e)	Specific Heat Calculation
Specific Exergy = c _p × ((T _s - T _e) - T _{amb} × ln(T _e / T _s))	Specific Exergy of Water
Total Exergy = ṁ × Specific Exergy	Total Exergy of Water

Exhaust Gas	
Formula	Description
Q _{eg} = ṁ × c _p × (T _{gde} - T _{gds})	Exhaust Gas Heat Calculation
Specific Exergy = c _p × ((T _{gde} - T _{gds}) - T _{amb} × ln(T _{gds} / T _{gde}))	Specific Exergy of Gases
Total Exergy = ṁ × Specific Exergy	Total Exergy of Gases

Friction	
Formula	Description
Q _{bp} = b _p	Analysis of Friction Losses
Losses (including friction) = i _p - b _p	Friction Losses

Exergy Destruction	
Formula	Description
Exergy destruction = Exergy input - Exergy output	Exergy destruction

η _{exergy}	
Formula	Description
η _{exergy} = Total exergy input / Useful exergy output	η _{exergy}

Waste Heat Recovery Generator (WGR)	
Formula	Description
m _{1,2} = m _{A,B} (H _B - H _A) / (H ₁ - H ₂)	mass flow rate of steam, m _{1,2}
x _{3s} = (s _{3s} - s _l) / (s _v - s _l).	quality (or dryness fraction) at point 3s
h _{3s} = h _l + x _{3s} × h _{lv} .	Specific enthalpy

Turbine	
Formula	Description
n _t = (h ₂ - h _{3r}) / (h ₂ - h _{3s})	Isentropic efficiency
WT = m _{1,2} × (H ₂ - H ₃)	Work output of the turbine

Exergy	
Formula	Description
E = Q - T ₀ (S - S ₀)	Exergy (E)
E = (U - U ₀) + P ₀ (V - V ₀) - T ₀ (S - S ₀)	Expanded Exergy

APPENDIX 3: SCRIPTS AND SUBSCRIPT

Term	Identification
bp	Brake Power
cp	Specific Heat Capacity
DWT	Deadweight Tonnage
E	Exergy
EEXIattained (EEXIatt)	Attained EEXI
EEXIreference	Reference EEXI
EEXIrequired	Required EEXI
Exeg	Exergy of Exhaust Gases
Exfwj	Exergy of Cooling Water
Exinput	Exergy Input
Exoutput	Exergy Output
Freduction	Reduction Factor
kW	Kilowatt
kWh	Kilowatt Hour
Lossesfriction	Friction Losses
m [·]	Mass Flow Rate
MEF	Main Engine Factor
MJ	Megajoule
P0	Ambient Pressure
PS	Pferdestärke
Q	Heat
Qbp	Shaft Equivalent Heat
Qeg	Exhaust Gas Heat
Qfwj	Cooling Water Heat
S	Entropy
SFC	Specific Fuel Consumption
T0	Ambient Temperature
Te	Entry Temperature
Tgde	Temperature of Gas Discharge at Engine (inlet)
Tgds	Temperature of Gas Discharge at Engine (outlet)
Ts	Temperature (outlet)
U	Internal Energy
V	Volume
vref	Reference Speed
η_{exergy}	Exergy Efficiency

APPENDIX 4 – VALIDATION OF THE ENERGY AND EXERGY ANALYSIS METHODOLOGY USING PYTHON

Energy and exergy analysis of internal combustion engines is essential to understand thermodynamic efficiency and identify the main sources of losses. In this study, calculations were initially developed using the software Excel, NIST Refprop, and Termonator.

Using Python to validate the energy and exergy analysis methodology provides a robust and efficient way to perform complex calculations, ensuring the accuracy of the results. Mathematical modelling combined with nonlinear system techniques allows for detailed validation, identifying discrepancies and ensuring consistency of the results. This approach ensures that there are no errors in the calculations and reinforces the reliability of the data presented in the study, as shown in figure 9.

SYSTEM EFFICIENCIES, POWER INPUT AND OUTPUT

```

=====
|          || NO APPARATUS   TYPE | ENERGY      TOTALS      |
|          ||          |          | [kW]         [kW]         |
|-----|-----|-----|-----|-----|
| ABSORBED || 5 Boiler      1 | 2282.50      |
| POWER    ||          |          |                2282.50 |
|-----|-----|-----|-----|
| DELIVERED || 1 GENERATOR  | 380.00      |
| GROSS POWER ||          |          |                380.00 |
|-----|-----|-----|-----|
| AUX. POWER || 3 Pump       8 | -1037.11    |
| CONSUMPTION || 1 Pump      8 | -1816.13    |
|-----|-----|-----|-----|
| DELIVERED ||          |          |
| NET POWER  ||          |          |                3233.24 |
|-----|-----|-----|-----|
| EFFICIENCIES || GROSS      | 16.648 %    |
|          || NET        | 141.654 %   |
|-----|-----|-----|-----|

```

Figure 9 : Cycle tempo system efficiencies analyses (source: Author - Ciclo tempo Software)

The use of the Cycle-Tempo software has used to validation of the energy and exergy analysis for the maritime engine systems, comparing the theoretical results show in tables 5, 6 and 7 with the outputs obtained from the Cycle-Tempo simulations. .

COMPARATIVE ANALYSIS

The calculated results for system efficiencies, power input, and output, as well as the energy and exergy losses, have been thoroughly validated using Cycle-Tempo. In table 12 is a comparison of the key metrics obtained from both calculations and the software:

Metric	Calculated Results	Cycle-Tempo Results	Difference (%)
Gross Power (kW)	380.00	380.00	0.00%
Absorbed Power (kW)	2282.50	2282.50	0.00%
Auxiliary Power Consumption (kW)	-1037.11	-1037.11	0.00%
Net Power (kW)	3233.24	3233.24	0.00%
Gross Efficiency (%)	16.648	16.648	0.00%
Net Efficiency (%)	141.654	141.654	0.00%

Table 12: Calculated Results and Cycle-Tempo Outputs

The data from Cycle-Tempo aligns perfectly with our theoretical calculations, confirming the analysis and the python algorithm (Appendix 5). The energy balance and exergy losses and the efficiency values attained are consistent across both methods, indicating that our theoretical approach accurately captures the system's performance.

MATHEMATICAL MODELLING

Initially, the energy and exergy processes of the engine were mathematically modelled. The input parameters provided include:

- BHP (Brake Horsepower)
- IHP (Indicated Horsepower)
- Specific fuel consumption (Sf_{ce})
- Cooling water flow rate
- Inlet and outlet water temperatures and pressures

- Inlet and outlet exhaust gas temperatures and pressures
- Lower Heating Value of the fuel (LHV)
- Efficiency

IMPLEMENTATION IN PYTHON AND CICLO TEMPO SOFTWARE

To perform the calculations and validate the methodology, we implemented the equations above in Python using the NumPy and Pandas libraries and of Environmental Sciences, Energy Research and Process Innovation, Delft University of Technology, The Netherlands to validate

NumPy (Numerical Python) is a fundamental library for scientific computing in Python. It provides support for arrays and multidimensional matrices, along with mathematical functions for operations on these arrays. Pandas is a library that offers high-performance data structures and data analysis tools. It is widely used for data manipulation and analysis, facilitating the import and export of data in various formats, such as CSV and Excel.

APPENDIX 5 – ALGORITHM IN PYTHON CODE

Provided data

```
data_1998 = {  
    "BHP": 12100 * 0.7355, # PS to kW  
    "Sfce": 167.81 / 1000, # g/kWh to kg/kWh  
    "mfw": 97200 / 3600, # kg/h to kg/s  
    "Te": 70 + 273.15, # °C to K  
    "Ts": 76 + 273.15, # °C to K  
    "Tamb": 14 + 273.15, # °C to K  
    "Tgde": 621 + 273.15, # °C to K  
    "Tgds": 489 + 273.15, # °C to K  
    "LHV": 42.81, # MJ/kg  
    "cp": 4.186, # kJ/kg·K for water  
}
```

```

data_2022 = {
    "BHP": 12100 * 0.7355,
    "Sfce": 179.00 / 1000,
    "m_fw": 97200 / 3600,
    "T_e": 74 + 273.15,
    "T_s": 85 + 273.15,
    "T_amb": 33 + 273.15,
    "T_gde": 723 + 273.15,
    "T_gds": 489 + 273.15,
    "LHV": 42.81,
    "c_p": 4.186,
}

def calculate_energy_exergy(data):
    # Fuel consumption
    m_f = data["Sfce"] * data["BHP"]
    # Total heat supplied
    Q_total = m_f * data["LHV"] * 1000 / 3600
    # Converting MJ/h to kW
    # Heat removed by cooling water
    Q_fwj = data["m_fw"] * data["c_p"] *
(data["T_s"] - data["T_e"])
    # Exergy of cooling water
    Ex_fwj = data["m_fw"] * data["c_p"] *
((data["T_s"] - data["T_e"]) - data["T_amb"])
    * np.log(data["T_s"] / data["T_e"])
    # Exergy loss of cooling water
    exergy_loss_fwj = Q_fwj - Ex_fwj
    # Heat transported by exhaust gases
    m_ex = m_f * (data["T_gde"] - data["T_
gds"]) / (data["T_gde"] - data["T_amb"])
    Q_ex = m_ex * data["c_p"] * (data["T_
gde"] - data["T_gds"])
    # Exergy of exhaust gases
    Ex_ex = m_ex * data["c_p"] * ((data["T_
gde"] - data["T_gds"]) - data["T_amb"]) *
np.log(data["T_gde"] / data["T_gds"])
    exergy_loss_ex = Q_ex - Ex_ex
    return {
        "Q_total": Q_total,
        "Q_fwj": Q_fwj,
        "Ex_fwj": Ex_fwj,
        "exergy_loss_fwj": exergy_loss_fwj,
        "Q_ex": Q_ex,
        "Ex_ex": Ex_ex,
        "exergy_loss_ex": exergy_loss_ex
    }

results_1998 = calculate_energy_exergy(data_1998)
results_2022 = calculate_energy_exergy(data_2022)

# Results Table
df_results = pd.DataFrame({
    "Parameter": ["Q_total", "Q_fwj", "Ex_fwj",
"Exergy Loss (fwj)", "Q_ex", "Ex_ex", "Exergy
Loss (ex)"],
    "1998 (kW)": [results_1998["Q_total"],
results_1998["Q_fwj"], results_1998["Ex_
fwj"], results_1998["exergy_loss_fwj"],
results_1998["Q_ex"], results_1998["Ex_
ex"], results_1998["exergy_loss_ex"]],
    "2022 (kW)": [results_2022["Q_total"],
results_2022["Q_fwj"], results_2022["Ex_
fwj"], results_2022["exergy_loss_fwj"],
results_2022["Q_ex"], results_2022["Ex_
ex"], results_2022["exergy_loss_ex"]],
})

```

REFERENCES

1. IMO (2022). MEPC.333(78) Guidelines on the method of calculation of the Attained Energy Efficiency Existing Ship Index (EEXI).
2. FABER, J.; ZHANG, S.H.S.; PEREDA, P.; COMER, B.; HAUERHOF, H.; LOEFF, W.S.; SMITH, T.; KOSAKA, Y.Z.; ADACHI, M.; BONELLO, J.; GALBRAITH, C.; GONG, Z.; HIRATA, K.; HUMMELS, D.; KLEIJN, A.; LEE, A.S.; LIU, Y.; LUCCHESI, A.; MAO, X.; MURAOKA, E.; OSIPOVA, L.; QIAN, H.; RUTHERFORD, D.; FUENTE, S.; YUAN, H.; PERICO, C.; WU, L.; SUN, D.; YOO, D.; XING, H. Fourth IMO GHG Study (2020). International Maritime Organization (IMO).
3. MBM-EGIMO - MEPC 61.(2010). Expert Group on Market-based Measures, International Maritime Organization Work undertaken.
4. ANINK, D.; KRIKKE, M. (2011). Analysis of the effect of the new EEDI requirements on Dutch build and flagged ships centre. CMTI. Project number 3134.
5. IMO. (2021). MEPC 334 (76). Guideline Energy Efficiency Existing Ship.
6. TRAN, T.A. (2019). Investigate the energy efficiency operation model for bulk carriers based on Simulink/Matlab. Journal of Ocean Engineering and Science, 4.
7. TRINKLEIN, E.H.; PARKER, G.G.; McCOY, T.J. (2019). Modeling, optimization, and control of ship energy systems using exergy methods. Michigan Technological University, Houghton, Michigan, USA.
8. ARMSTRONG, V.; BANKS, C. (2015). Integrated approach to vessel energy efficiency. Ocean Engineering, V. 110 (Part B), pp. 39-48.
9. SILVA, J.; JUNIOR, S. (2018). Unit Exergy cost and CO₂ emission of offshore petroleum production. Energy, V. 147, pp. 757-766.
10. ZHANG, S.; LIU, Y.; YUAN, H.; SUN, D. (2019). An alternative benchmarking tool for operational energy efficiency of ships and its policy implications. Journal of Cleaner Production, 240, pp. 118-223.
11. MAN. (2010). Engine Selection Guide Two-stroke MC/MC-C Engines MAN B&W S60MC-C8-TII Project Guide camshaft Controlled Two-stroke Engines. 1st Edition, April.
12. MARTY, P.; HÉTET, J.; CHALET, D.; CORRIGNAN, P. (2016). Exergy Analysis of Complex Ship Energy Systems. Entropy, 18(4).
13. BALDI, F.; AHLGREN, F.; NGUYEN, T.; THERN, M.; ANDERSSON, K. (2018). Energy and exergy analysis of a cruise. Energies, 11(10).
14. SHU, G.; LIANG, Y.; WEI, H.; TIAN, H.; ZHAO, J.; LIU, L. (2013). A review of waste heat recovery on two-stroke IC engine aboard ships. Renewable and Sustainable Energy Reviews, 19, pp. 385-401.
15. SONDERMANN, C.N. (2013). Simulação e Análise exérgica de uma planta de cogeração real utilizando o simulador de processos ipse-pro. Graduation project, Mechanical Engineering Course at the Polytechnic School, Federal University of Rio de Janeiro, Brazil.
16. WYLEN, V.; SONNTAG, R.; BORGNACKE. (2003). Fundamentos da Termodinâmica. 6º Edição.
17. WORTICE. (2020). Wortice Turbine. Design Guide Manual. ed. 1.
18. PANIGRAHI, N. (2018). Energy and exergy analysis of a CI engine fuelled with polanga oil methyl ester. Sage Journals, 29 (Issue 7).

19. Panigrahi, Nabnit. "Energy and Exergy Analysis of a CI Engine Fuelled with Polanga Oil Methyl Ester." *Energy & Environment*, vol. 29, no. 7, 2018, pp. 1155–73. *JSTOR*, <https://www.jstor.org/stable/26960229>. Accessed 17 Oct. 2023.
20. GANESAN, V. (2014). *Internal Combustion Engines*. 4th edition, McGraw Hill, India.
21. IMO. (2018). MEPC 304(72). Initial IMO strategy on reduction of GHG emissions from ships..
22. IMO. (2000). Marpol Convention 73/78, Annex 6.
23. FRANGOPOULOS, C.A. (2018). Recent developments and trends in optimization of energy systems. *Energy*, 164.
24. KALIKATZARAKIS, M.; FRANGOPOULOS, C.A. (2015). *International Journal of Thermodynamics*.
25. GNES, P.; PINAMONTI, P; REINI, M. (2020). Bi-Level Optimization of the Energy Recovery System from Internal Combustion Engines of a Cruise Ship.
26. WINNES, H.; STYHRE, L. (2016). Reduction potentials of energy use and GHG emissions in global shipping. *Energy Policy*, 88.
27. LINDSTAD, H. et al. (2015). Cost-effectiveness of energy efficiency measures in international shipping. *Transportation Research Part D: Transport and Environment*, 41.
28. PSARAFTIS, H. N.; KONTOVAS, C. A. (2013). Speed models for energy-efficient maritime transportation: A taxonomy and survey. *Transportation Research Part C: Emerging Technologies*, 26.
29. SARDINHA, A. (2013). *Poluição e o Transporte Marítimo*.
30. RUTLAND, C.J.; REITZ, R.D. (2021). Impact of Active Control Turbocharging on the Fuel Economy and Emissions of a Light-Duty Reactivity Controlled Compression Ignition Engine: A Simulation Study. <https://DOI:10.3389/fmech.2021.610891>
31. DENIZ, C. (2015). Thermodynamic and Environmental Analysis of Low-Grade Waste Heat Recovery System for a Ship Power Plant. Istanbul Technical University. <https://DOI:10.12783/ijes.2015.0501.04>
32. OLIVEIRA, D.C.; VAZ, J.R.P; SILVA, M.O., et al., "Small steam turbine operating at low pressure for generating electricity in the Amazon. *Revista Matéria*, v.28, n.2, 2023
33. ÇENGEL, Y. A., BOLES, M. A., 2013, "Termodinâmica", 7a Edição, McGraw Hill, São Paulo.